

DOE/MC/08216-1331
(DE83006486)

HYDRAULIC FRACTURING EXPERIMENTS IN
DEVONIAN SHALE AND PRE-FRACTURED
HYDROSTONE

September 30, 1981

Work Performed Under Contract No. AM21-78MC08216

For
Morgantown Energy Technology Center
Morgantown, West Virginia

By
Science Applications, Inc.
Steamboat Springs, Colorado

TECHNICAL INFORMATION CENTER
UNITED STATES DEPARTMENT OF ENERGY

DISCLAIMER

"This report was prepared as an account of work sponsored by an agency of the United States Government. Neither the United States Government nor any agency thereof, nor any of their employees, makes any warranty, express or implied, or assumes any legal liability or responsibility for the accuracy, completeness, or usefulness of any information, apparatus, product, or process disclosed, or represents that its use would not infringe privately owned rights. Reference herein to any specific commercial product, process, or service by trade name, trademark, manufacturer, or otherwise, does not necessarily constitute or imply its endorsement, recommendation, or favoring by the United States Government or any agency thereof. The views and opinions of authors expressed herein do not necessarily state or reflect those of the United States Government or any agency thereof."

This report has been reproduced directly from the best available copy.

Available from the National Technical Information Service, U. S. Department of Commerce, Springfield, Virginia 22161.

Price: Printed Copy A04
Microfiche A01

Codes are used for pricing all publications. The code is determined by the number of pages in the publication. Information pertaining to the pricing codes can be found in the current issues of the following publications, which are generally available in most libraries: *Energy Research Abstracts, (ERA)*; *Government Reports Announcements and Index (GRA and I)*; *Scientific and Technical Abstract Reports (STAR)*; and publication, NTIS-PR-360 available from (NTIS) at the above address.

HYDRAULIC FRACTURING EXPERIMENTS
IN
DEVONIAN SHALE
AND
PRE-FRACTURED HYDROSTONE

by

Thomas L. Blanton

FINAL REPORT

September 30, 1981

Prepared For

Eastern Gas Shales Project
Morgantown Energy Technology Center
Collins Ferry Road
Morgantown, West Virginia 26505

Contract No. DE-AM21-78MC08216
Year III, Mod 7, Activity 3

Prepared by

Science Applications, Inc.
P.O. Box 880010
Steamboat Springs, Colorado 80488

TABLE OF CONTENTS

EXECUTIVE SUMMARY	1
SECTION 1. INTRODUCTION.	3
SECTION 2. EXPERIMENTS	5
2.1 Triaxial Compression Apparatus	5
2.2 Specimen Preparation.	10
2.3 Experimental Conditions.	11
2.4 Results of Tests in Pre-Fractured Hydrostone.	11
2.5 Results of Tests in Devonian Shale	23
SECTION 3. ANALYSIS	31
3.1 Theoretical Considerations.	31
3.2 Compression Between Theory and Experiment.	35
SECTION 4. CONCLUSION	43
ACKNOWLEDGEMENTS	44
REFERENCES	45
APPENDIX A: Pressure-Time Plots for Tests in Pre-fracture Hydrostone	46
APPENDIX B: Pressure-Time Plots for Tests in Devonian Shale.	57

EXECUTIVE SUMMARY

The Devonian shale reservoirs in the Appalachian Basin are naturally fractured reservoirs, and constructive interaction with the natural fracture system is critical to the success of any stimulation treatment. To be effective hydraulic fractures should cross and connect the natural fracture system, but it is possible that arrest, diversion, or offset could occur thus inhibiting fracture growth and proppant placement. The purpose of this study has been to perform laboratory experiments that allow examination of hydraulic fracture propagation in pre-fractured material under triaxial states of stress. Tests have been run on naturally fractured blocks of Devonian shale as well as blocks of hydrostone in which planar fractures have been created. Specific objectives were to (1) qualitatively examine the effect of natural fractures on the morphology of hydraulic fractures in Devonian shale and (2) determine under what combination of stresses and angle of approach a hydraulic fracture will cross a pre-existing fracture.

The experiments were performed in a triaxial compression apparatus capable of subjecting a 12 x 12 x 15-inch (30 x 30 x 38 cm) block to magnitudes of stress up to 3,000 psi (~20 MPa). Hydraulic fractures were initiated from a central eighth-inch borehole with a one-inch-long open-hole section. Upon completion of a test the block was sectioned, and observations and measurements of the resulting hydraulic fracture were made.

In tests on pre-fractured hydrostone the hydraulic fracture was able to cross the pre-fracture only at high angles of approach and under high horizontal differential stresses. In most cases either the pre-fracture opened and the fracturing fluid was diverted down the pre-fracture or the hydraulic fracture was arrested by the pre-fracture and continued to grow in the other direction.

Tests in Devonian shale blocks also showed the strong influence of pre-existing fractures. Diversion of fracturing fluid, fracture arrest, and branching were all observed in the hydraulically fractured blocks. These phenomena tended to occur in tests with lower horizontal differential stress.

Conceivably three things can happen when a hydraulic fracture intersects a pre-existing fracture: it can open the pre-existing fracture, it can be arrested by the pre-existing fracture, or it can cross the pre-existing fracture. Simple criteria for when each of these should happen have been developed based on the pressure in the hydraulic fracture and the normal and shear stresses on the pre-existing fracture. The criteria indicate that for most realistic combinations of horizontal differential stress and angle of approach the hydraulic fracture will be truncated by the pre-fracture with either the pre-fracture opening and taking fluid or simply arresting the hydraulic fracture. Thus, theory tends to confirm the strong influence of pre-existing fractures suggested by the experiments.

The implication of both theory and experiment for hydraulic fracturing in the field is that symmetrical, double-winged, vertical fractures are probably rare occurrences in naturally fractured reservoirs. It would be more likely to have fractures with wings diverted at different angles or with truncated wings of different lengths.

SECTION 1. INTRODUCTION

The Devonian shale reservoirs in the Appalachian Basin are naturally fractured reservoirs, and interaction with the fracture system is critical to the success of any stimulation treatment, be it hydraulic, explosive, or tailored-pulse-loading. In April 1980, SAI, with the support of METC, conducted a workshop to determine the state-of-the-art in stimulation of naturally fractured reservoirs with participants representing government, academic, and industry institutions. Numerical and experimental work presented at the workshop which treated the interaction of induced and existing fractures was primarily concerned with the problem of an induced fracture approaching an existing discontinuity at right angles with the existing discontinuity under simple normal load. The problems of induced fractures propagating at angles to existing fractures under triaxial states of stress had not been adequately addressed. Moreover, field observations presented at the workshop suggest that the opening of auxiliary fracture systems may be signaled by characteristics of the pressure/time record during a hydraulic fracturing treatment.

In order for hydraulic stimulation treatments to be effective in Devonian shales, the hydraulic fractures should cross and connect the natural fracture system. There are several situations in which the desired connectedness would not be obtained. The fracturing fluid may simply open existing fractures without creating any new connectedness, or natural fractures may act as barriers to propagation of the hydraulic fracture. Interaction between induced and existing fracture systems may also be detrimental to fracture conductivity. Existing fractures could cause offsets in the induced fracture which would impede proppant movement and upon closure cut off much of the fracture length from the wellbore. Another problem is that opening of auxiliary fracture systems can increase leak-off and concentrate proppant in the main fracture which can lead to plugging of the fracture. Ideally one would like the induced fracture to intersect the natural fracture system in a constructive way increasing fracture conductivity.

The purpose of this project has been to perform laboratory experiments which allow examination of hydraulic fracture propagation in

pre-fractured material under triaxial states of stress. Tests have been run on naturally fractured blocks of Devonian shale as well as blocks of hydrostone in which pre-fractures have been created. Specific objectives of the project have been as follows:

- To determine under what combination of stresses and angle of approach a hydraulic fracture will cross a pre-fracture.
- Qualitatively examine the effect of natural fractures on the morphology of hydraulic fractures in Devonian shale.

SECTION 2. EXPERIMENTS

2.1. Triaxial Compression Apparatus

To be useful in studying deep-penetrating hydraulic fractures at in situ stress conditions an experimental apparatus should have the following characteristics:

- A size that allows stable fracture propagation to occur over a distance that is large compared to the borehole diameter.
- A load capacity capable of generating stresses comparable to those encountered downhole.

To this end a 500,000-pound triaxial load frame has been constructed capable of subjecting a 12 x 12 x 15-inch (30 x 30 x 38-cm) block to magnitudes of stress up to 3,000 psi (~20 MPa). Cross-sectional diagrams of the apparatus are shown in Figures 1 and 2. Figure 3 shows the apparatus being assembled for a test.

The frame consists of a steel tube 22 inches in diameter and 15.1 inches high with a wall thickness of 1.5 inches. The tube is capped on top and bottom with 2-inch thick steel plates held together by 12 1-inch steel tie rods. The inner space for the test block is lined with an aluminum box and the space between the box and the steel tube is filled with concrete. Stresses are applied with three pairs of opposing flatjacks filled with hydraulic oil under pressure. A 0.5-inch steel spacer is placed between the test block and the upper flatjack to allow access to the borehole through a slot.

Two hydraulic systems, one for the flatjacks and one for the fracturing pressures, are used in running a test. These systems are illustrated schematically in Figure 4. Each pair of flatjacks is pressurized independently with a hydraulic pump. The fracturing pressure is generated by a pressure intensifier consisting of two opposing hydraulic rams, one with an 8-inch diameter piston and one with a 4-inch diameter piston. The intensifier is actuated by a closed-loop servo-control system that has as its feedback the output of an LVDT which

VERTICAL CROSS SECTION OF
TRIAXIAL COMPRESSION APPARATUS

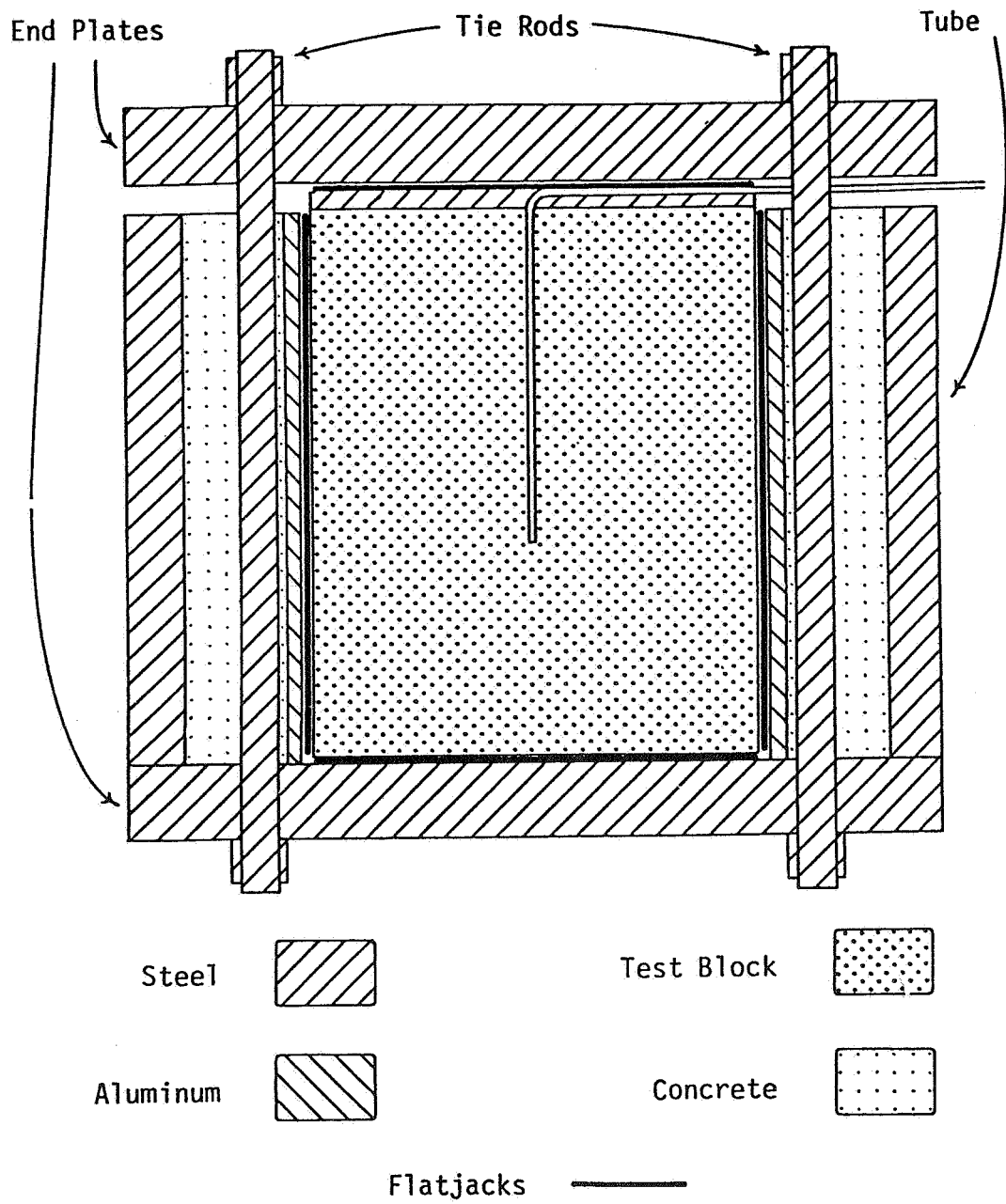


Figure 1. Vertical cross section of triaxial compression apparatus.

HORIZONTAL CROSS SECTION OF
TRIAXIAL COMPRESSION APPARATUS

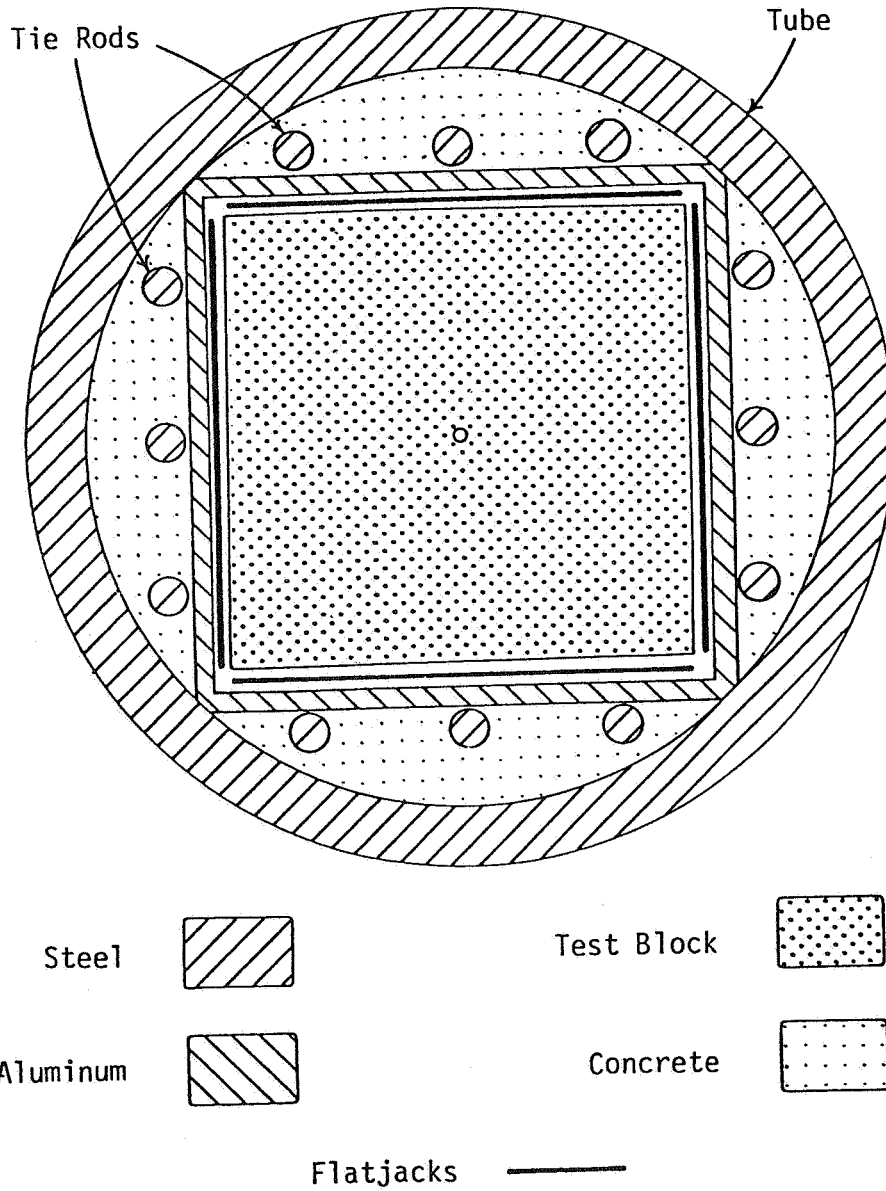


Figure 2. Horizontal cross section of triaxial compression apparatus.

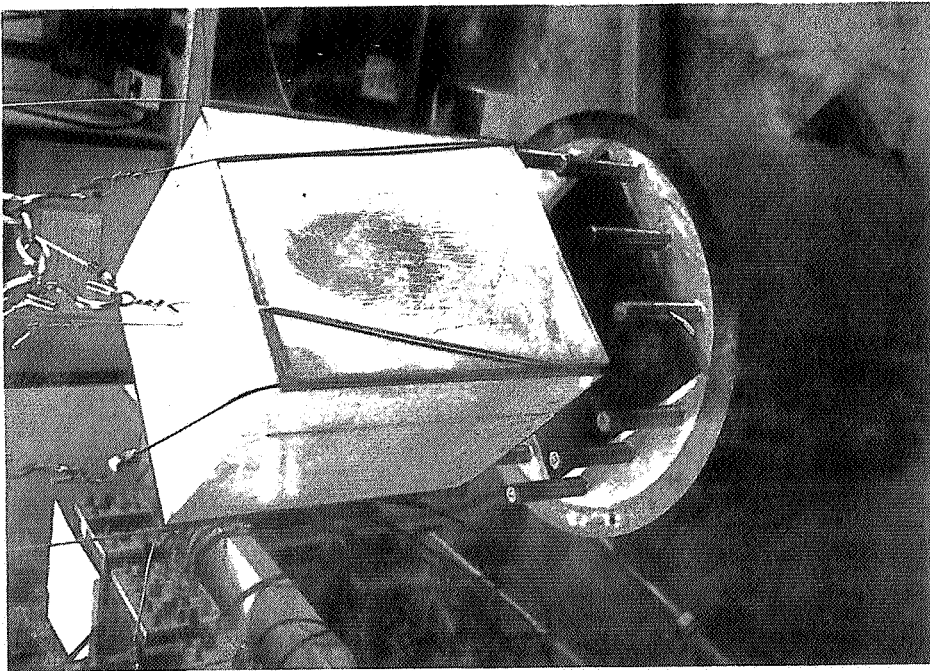
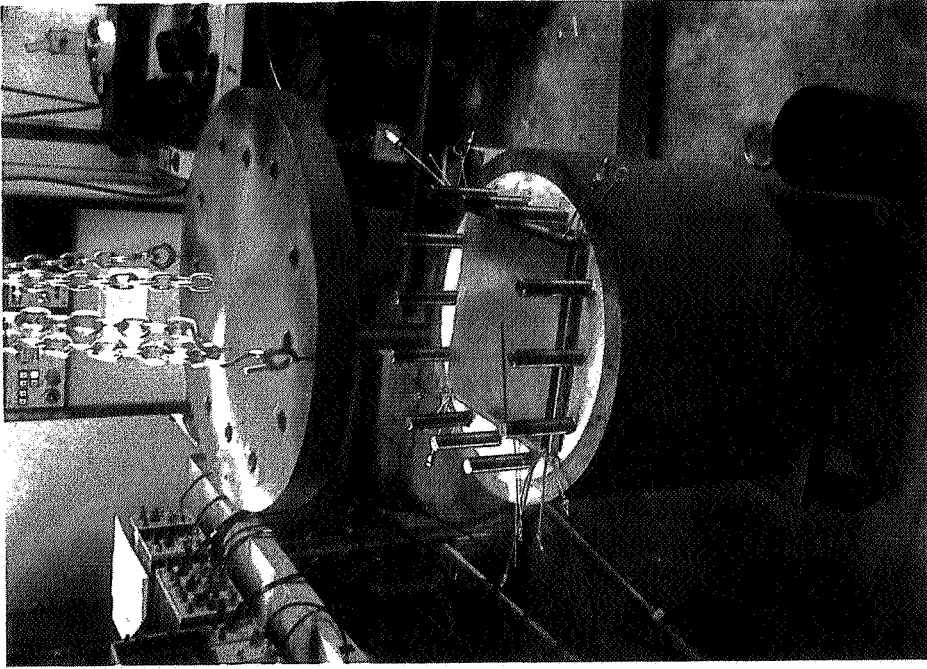


Figure 3. Assembly of apparatus for hydraulic fracturing experiment.

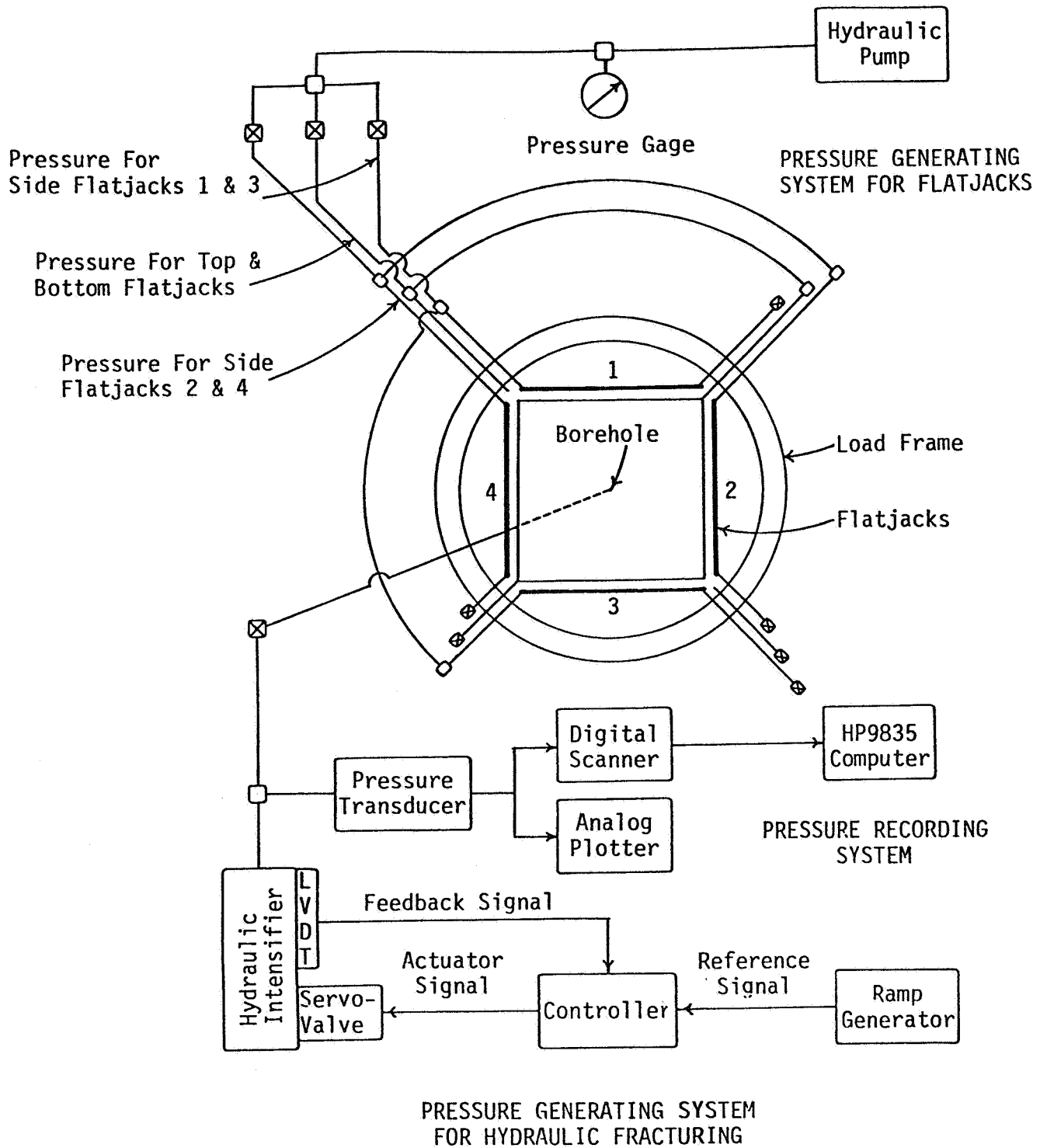


Figure 4. Schematic diagram of hydraulic fracturing test system.

measures the movement of the intensifier pistons. Since the diameter of the pistons is relatively constant the LVDT essentially measures volume changes. Using a ramp voltage for a reference signal causes the intensifier to displace fracturing fluid at a constant flow rate. Flow can be interrupted at any time during a test by placing the ramp generator on hold, for example to take an instantaneous shut-in pressure. Fracturing pressures are recorded in analog and digital form. The digital record is stored on tape for subsequent analysis and plotting with an HP 9835 desktop computer. After completing a test, the block is removed and sectioned with a 12-inch diamond saw in order to examine the fracture or fractures.

2.2. Specimen Preparation

To meet the objectives stated in the introduction tests have been run on two types of blocks: hydrostone and Devonian shale.

Hydrostone has been used so that the angle between the hydraulic fracture and the pre-fracture can be varied in a systematic way. These blocks are prepared in a mold 30 x 30 x 38 cm (12 x 12 x 15 inches). To create a fracture at a given angle, the mold is first placed with its long dimension parallel to the floor and then tilted at the prescribed angle. Hydrostone is then poured to a level that is about 2.5 cm (1 inch) from where the central wellbore will eventually be drilled. After this initial pouring sets, the surface is sprayed with a light lubricant, and the remainder of the mold is filled with hydrostone. When the final pouring sets, the block is removed from the mold and tapped with a rubber hammer. This causes the block to part on the lubricated surface. A central 1/8-inch hole is drilled to a depth of 20 cm (8 inches) parallel to the long dimension of the block. Steel tubing is then epoxied in the hole to a depth of about 17.5 cm (7 inches), leaving a central 2.5-cm (1-inch) open-hole section.

It may be argued that the lubricant will affect the interaction of the pre-existing and hydraulic fracture. In fact it will, as the coefficient of friction has been shown to be important in earlier work

(Hanson, et al., 1981). However, what we are concerned with here is that the coefficient of friction is consistent from experiment to experiment.

Shale blocks were prepared from boulders obtained from the Mound Facility. Cuts were made perpendicular to the bedding planes to form blocks measuring 29 x 29 cm (11.5 x 11.5 inches) parallel to the bedding. The dimension perpendicular to bedding varied from 20 to 25 cm (8 to 10 inches) from block to block because of a tendency for the shale to part on bedding planes. These blocks were then cast in hydrostone to bring the dimensions to 30 x 30 x 38 cm (12 x 12 x 15 inches). A hole was drilled and cased in the same manner as in the hydrostone blocks with the 2.5-cm (1-inch) open-hole section central to the shale portion and perpendicular to bedding.

2.3. Experimental Conditions

The experimental conditions are listed in Tables 1 and 2. Multiple tests were run in all but one of the six hydrostone blocks by changing the magnitudes of the horizontal stresses. Two tests were run in each of blocks 2, 4, 5, and 6. This was done by reversing the directions of the maximum and minimum horizontal stresses after the first test so that the second hydraulic fracture propagated at right angles to the first. In the pre-fractured blocks this allowed either two different angles of approach under the same stresses, as in block 4, or the same angle of approach under differing stress conditions, as in blocks 5 and 6. An attempt was made to run four tests in block 3, but this led to questionable results as discussed in the next section. To avoid any confusion about the results in shale, only one test was run in each block.

2.4 Results of Tests in Pre-Fractured Hydrostone

The first three tests (CT-2, CT-3a, CT-3b) in hydrostone were run in solid blocks in order to observe fracture growth in the absence of pre-existing fractures. This provides a basis for comparison with

Table 1: Experimental Conditions for Tests in Hydrostone 35/100.

Block #	Test #	Pre-Fracture Orientation	Horizontal Stresses*(MPa)		Horizontal Differential Stress, $\sigma_{\max} - \sigma_{\min}$ (MPa)
			σ_{\max}	σ_{\min}	
1	CT-2	-	12	10	2
2	CT-3a	-	19	10	9
2	CT-3b	-	15	10	5
3	CT-4	60°	12	10	2
3	CT-5	60°	19	10	9
3	CT-6	60°	15	10	5
3	CT-7	30°	19	10	9
4	CT-8	60°	20	5	15
4	CT-9	30°	20	5	15
5	CT-11	45°	20	5	15
5	CT-12	45°	18	5	13
6	CT-13	45°	16	5	11
6	CT-14	45°	14	5	9

*Vertical stress was 20 MPa for all hydrostone tests.

Table 2. Experimental Conditions for Test in Devonian Shale

Test #	<u>Principal Stresses (MPa)</u>			Horizontal Differential Stress, $\sigma_{\max} - \sigma_{\min}$ (MPa)
	Vertical σ_v	Horizontal σ_{\max} σ_{\min}		
CT-10	20	20	5	15
CT-15	20	15	10	5
CI-16	20	10	5	5
CT-17	20	10	8	2

subsequent tests. The maximum and minimum principal stresses were 20 MPa and 10 MPa, respectively, for all three tests. The intermediate stress is different for each test, changing from 12 MPa to 15 MPa, and then to 19 MPa. The last two tests were run in the same block by reversing direction of the maximum and minimum horizontal stresses. The photographs in Figure 7 and the fracture dimensions listed in Table 3 show that a more symmetrical and more planar fracture developed when the horizontal differential stress was greater.

An attempt was made to run four tests in block 3. The intent was to create a hydraulic fracture that would first open the pre-existing fracture upon intersection and then in a second test under a different stress field cross the pre-existing fracture. This would be done for two angles of approach making four tests. In fact, none of the hydraulic fractures crossed the pre-existing fracture as can be seen in Figure 8.

In the first two tests (CT-4 and CT-5) the least principal stress was applied to the top and bottom of the block shown in Figure 8 so that the fracture for both instances approached the pre-existing fracture at 60° . Obviously the hydraulic fracture did not cross the pre-existing fracture in either test, and in at least one test fluid flow occurred along the pre-existing fracture. Fluid flow is most likely to have occurred in the test with the lowest normal stress across the pre-existing fracture, since this would be the condition for easiest opening by fluid pressure. The equation for normal stress, σ , across a plane at angle θ to σ_{\max} is:

$$\sigma = \sigma_{\max} \sin^2\theta + \sigma_{\min} \cos^2\theta \quad (1)$$

Values for normal stress have been calculated for each test and are shown in Table 3. Between the first two tests in block 3, CT-4 had the lowest normal stress, therefore, was the easiest to open. Whether or not CT-5 also opened the pre-fracture cannot be determined. It can only be said that it either opened the pre-fracture or was arrested by it. This uncertainty is reflected in Table 3.

The next two tests run in block 3 were intended to involve a

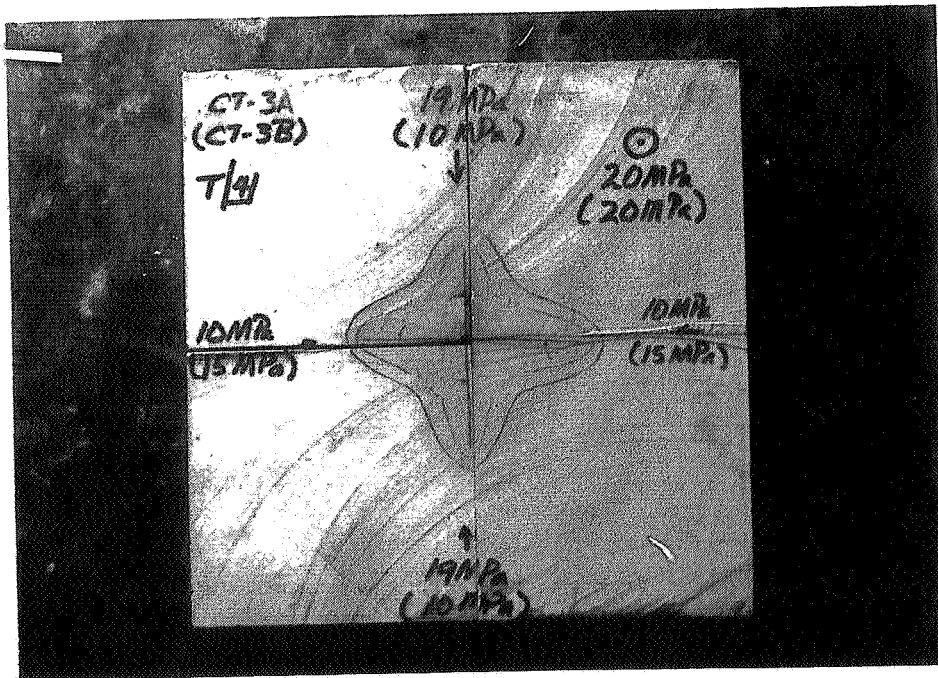
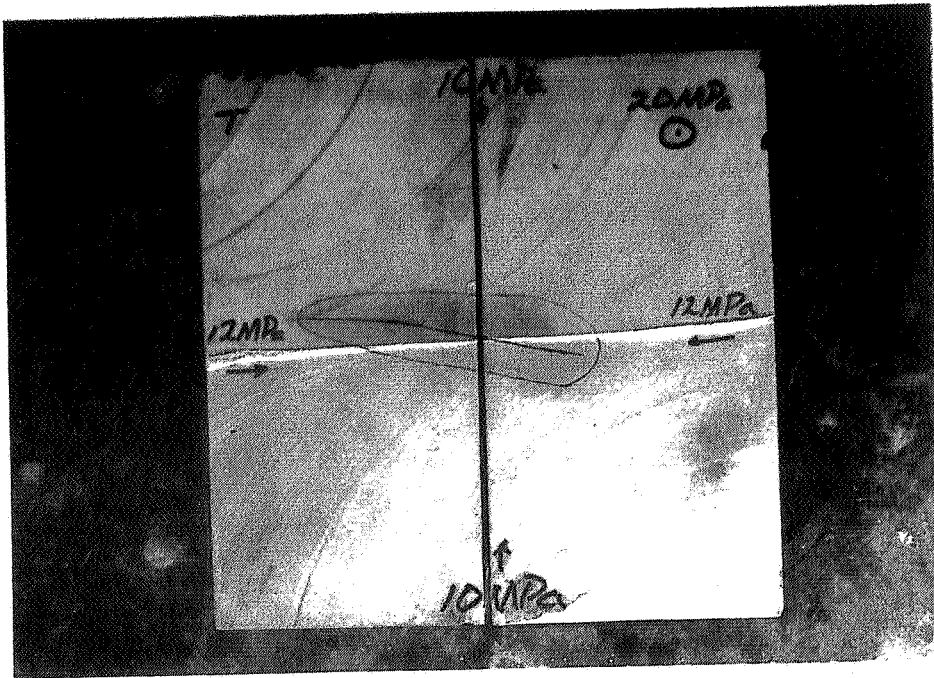


Figure 7. Tests CT-2, CT-3a, and CT-3b.

Table 3. Results of Tests in Hydrostone 35/100.

Block #	Test #	Stresses on Pre-Fracture (MPa)		Interaction with Pre-fracture	Hydraulic Fracture Dimensions (cm)		
		Normal	Shear		Height	Wing-Lengths	Wing-Lengths
1	CT-2	-	-	-	14.61	5.40	9.21
2	CT-3a	-	-	-	13.81	5.40	6.19
2	CT-3b	-	-	-	13.97	6.19	6.67
3	CT-4	11.50	0.87	open	15.08	12.70	1.59
3	CT-5	16.75	3.90	arrest (open?)	15.08	12.70	1.59
3	CT-6	13.75	2.17	arrest (open?)	15.08	12.70	1.59
3	CT-7	12.25	3.90	open	16.04	6.19	3.18
4	CT-8	16.25	6.50	cross	15.72	7.94	7.78
4	CT-9	8.75	6.50	arrest	N/A	10.95	6.35
5	CT-11	12.50	7.50	arrest	16.51	8.10	3.81
5	CT-12	11.50	6.50	arrest	20.96	8.73	3.81
6	CT-13	10.50	5.50	arrest	15.24	7.94	3.81
6	CT-14	9.50	4.50	arrest	17.15	11.11	3.81

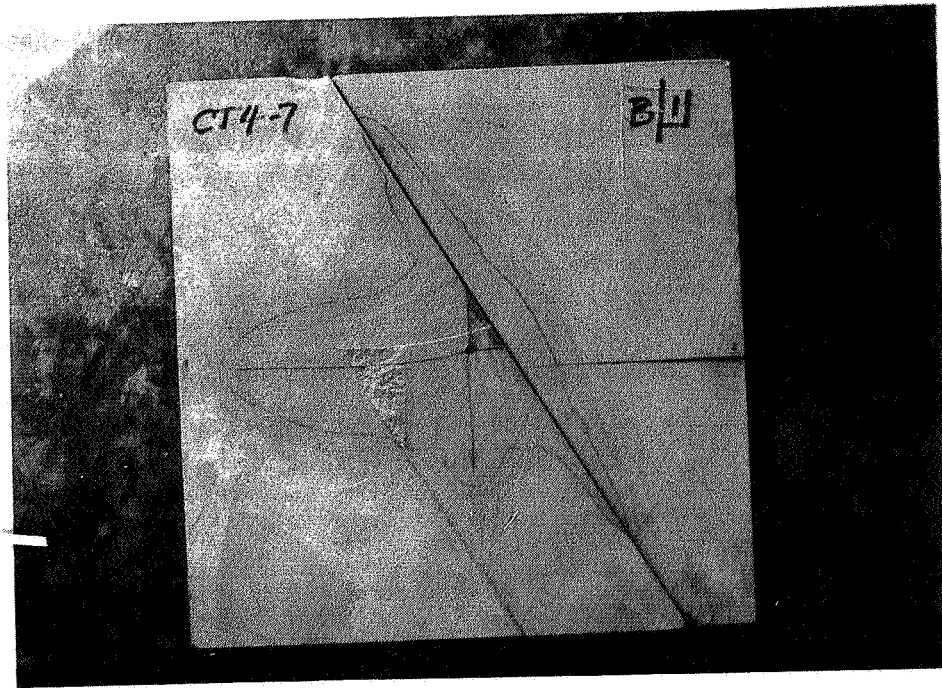


Figure 8. Tests CT-4 through CT-7.

hydraulic fracture at right angles to the first and approaching the pre-fracture at a 30° angle. However, three points of evidence suggest that CT-6 simply opened the existing hydraulic fracture rather than creating a new one. First, the fracture extension pressures for CT-4, CT-5, and CT-7 range from 12 MPa to 15 MPa (see pressure-time curves in Appendix A), whereas for CT-6 the range is 20 MPa to 22 MPa. The least principal stress for all tests was 10 MPa and the fracture extension pressures should have been only slightly above 10 MPa due to fluid friction pressure and tensile strength. The anomalously high fracture extension pressure in CT-6 suggests that the fluid pressure was opening a fracture against (perpendicular to) the maximum horizontal stress of 15 MPa. Second, the photograph in Figure 8 clearly shows that the fracture created by the first test took more fluid than the fracture at 90° to it. The fluid volumes were equal for all tests, and therefore if both fractures in Figure 8 had had two tests run in them, their extent should be more nearly equal. It is more probable that the longer fracture had three tests run in it (CT-4, CT-5 and CT-6) and the shorter fracture had only one test run in it (CT-7). Third, the breakdown pressure relative to the extension pressure for CT-6 was very low suggesting that there may not have been a "breakdown", but only an opening of an existing fracture.

The hydraulic fracture created in CT-7 approaching the pre-fracture at 30° was arrested by it and most probably opened it judging from the amount of fluid penetration (Figure 8).

The major conclusion from the test run in block 3 was that four tests are too many tests to run in one block. Subsequent work in hydrostone was restricted to two tests per block.

The tests run in block 4 provided examples of hydraulic fractures that either crossed or were arrested by a pre-fracture (Figures 9 and 10). The hydraulic fracture created in test CT-8 was the only one in the series that crossed a pre-fracture, and it was also the one with the highest normal stress across the pre-fracture (Table 3). In the remaining tests (CT-9 and CT-11 through CT-14) all the hydraulic fractures were arrested by the pre-fractures with little or no fluid penetration (Figures 9 through 12).

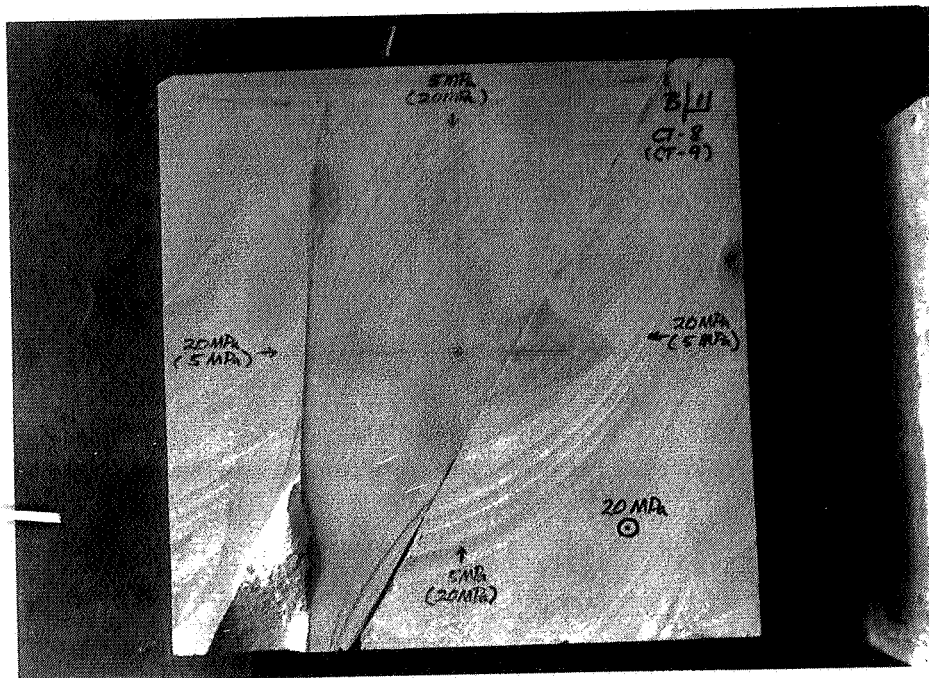


Figure 9. Tests CT-8 and CT-9.

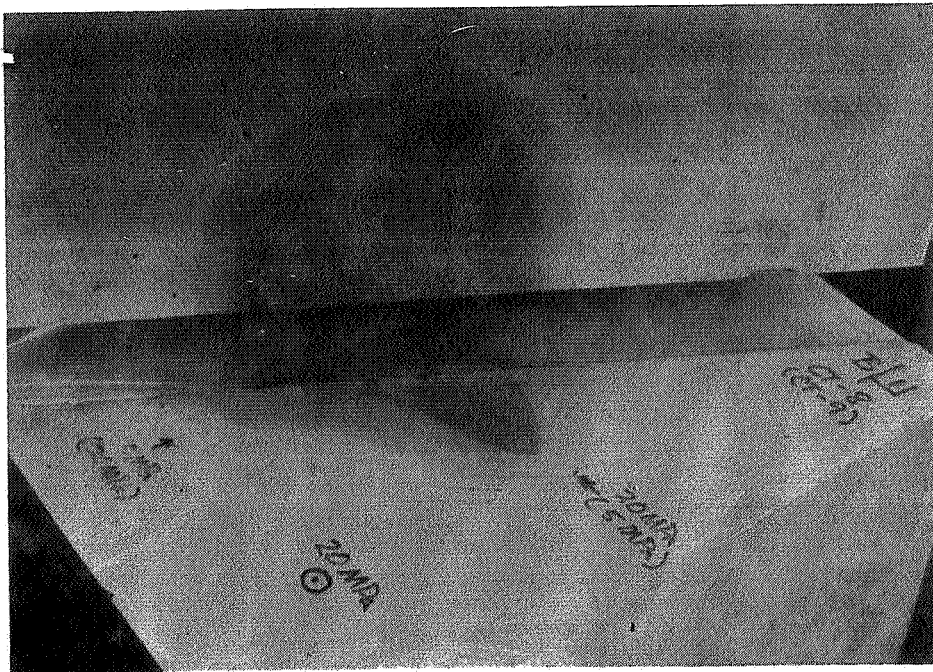
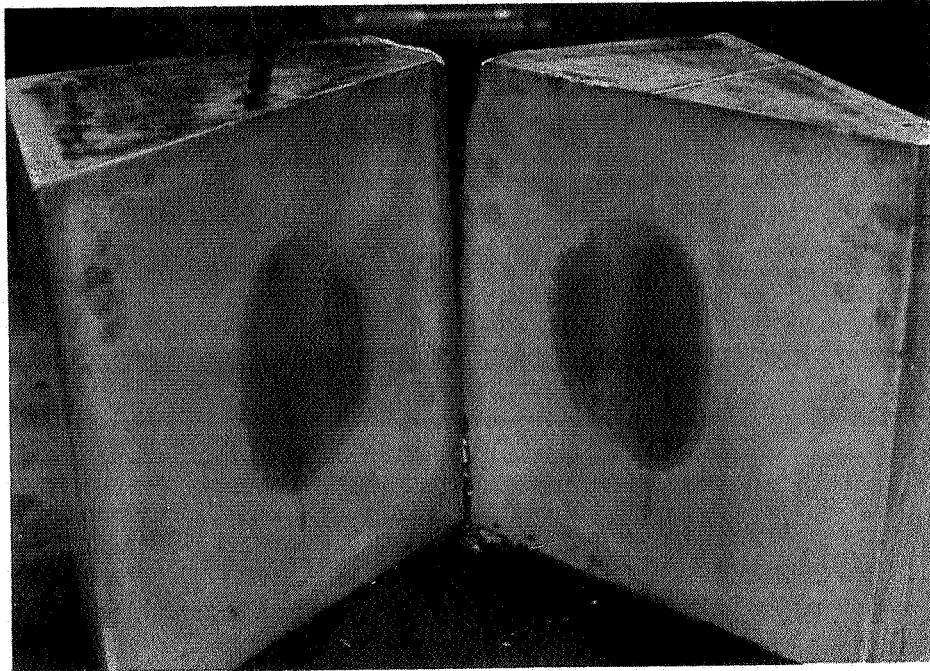


Figure 10. Vertical view of fractures created in tests CT-8 and CT-9.

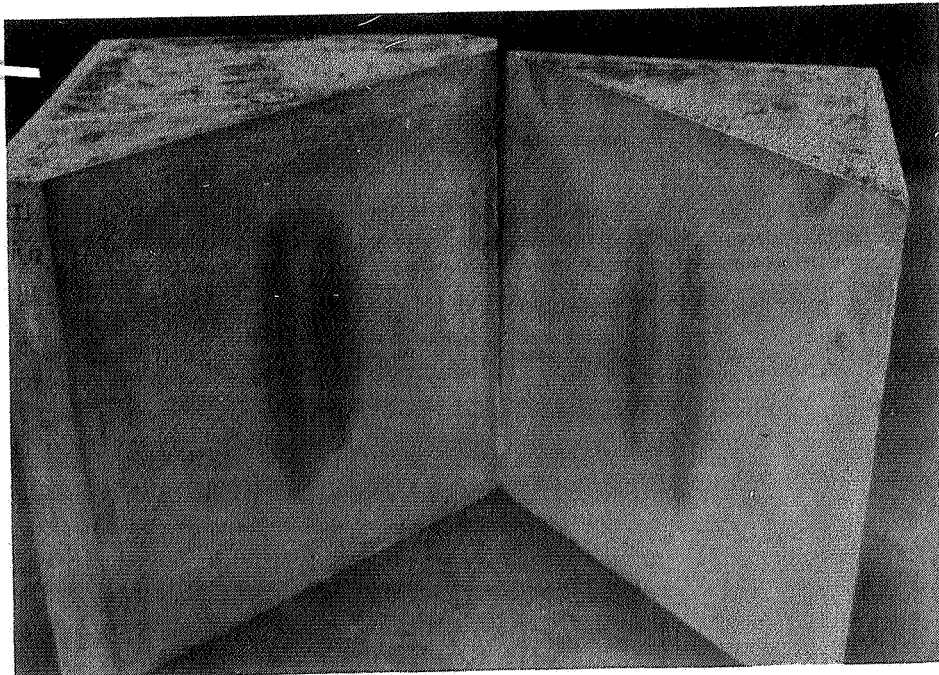
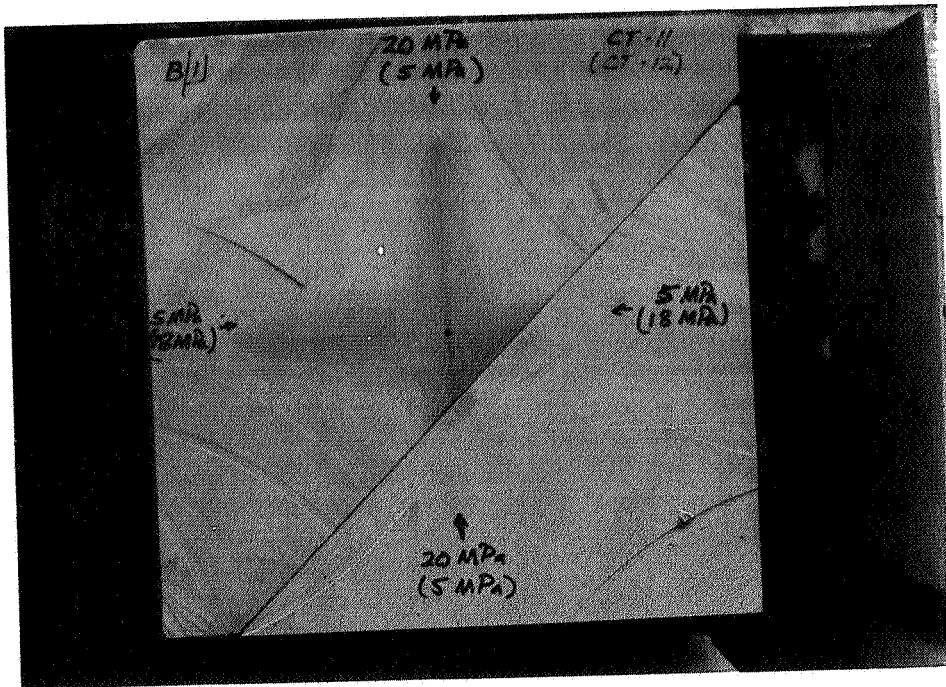


Figure 11. Tests CT-11 and CT-12.

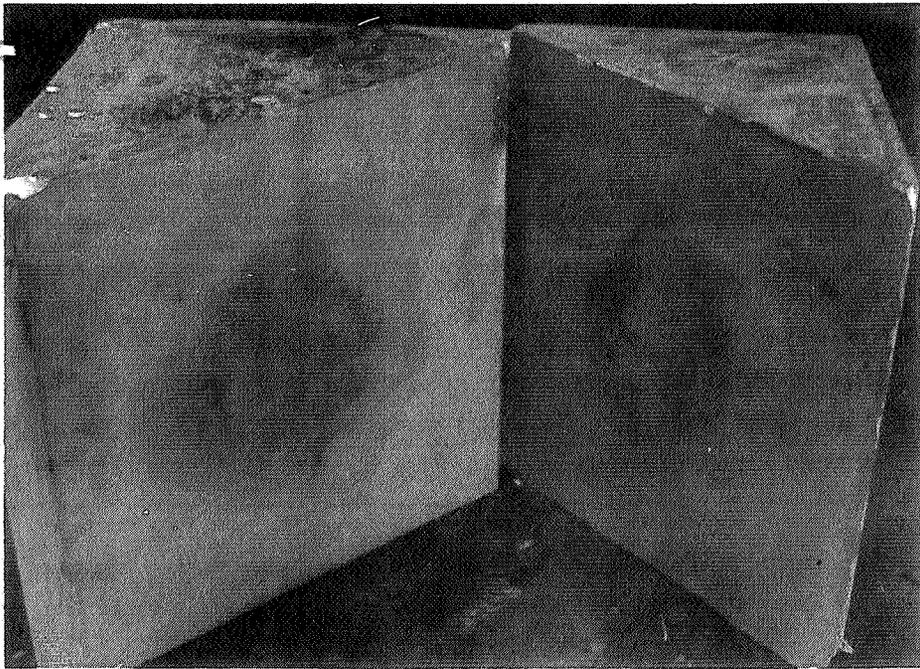
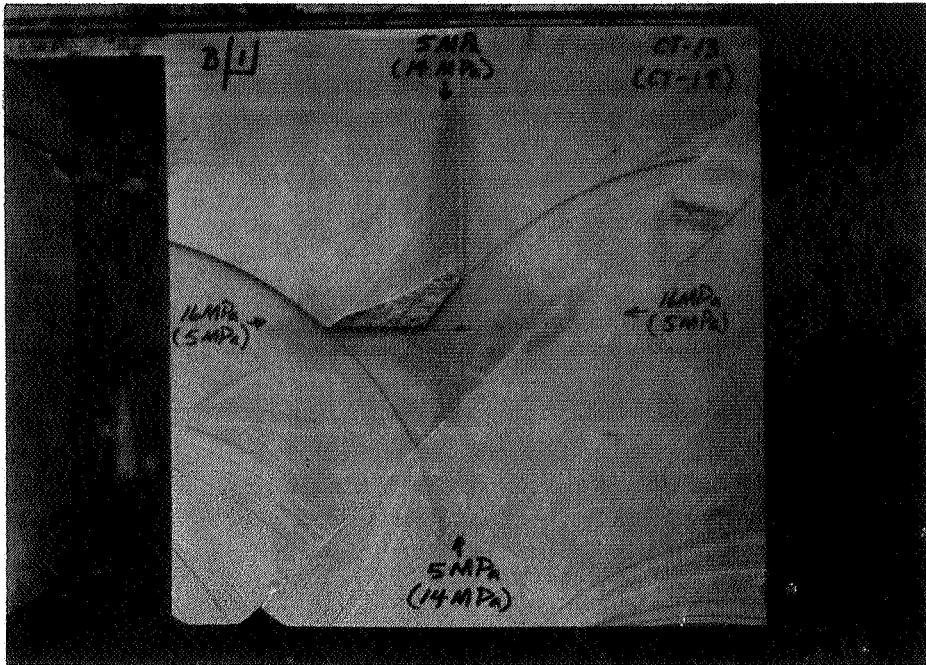


Figure 12. Tests CT-13 and CT-14

2.5. Results of Tests in Devonian Shale

The orientation and number of natural fractures in test blocks of Devonian shale could not be determined prior to a test, so the only controlled variables were the stresses applied to the boundaries. The vertical stress was 20 MPa in all four tests in order to clamp the bedding planes as much as possible. The horizontal stresses were varied so that the effect of changes in horizontal differential stress and mean stress could be examined. The mean stress for CT-10 and CT-15 is constant (15 MPa) while the differential stress is varied from 15 to 5 MPa (Table 2). For tests CT-15 and CT-16, the differential stress is the same (5 MPa) while the mean stress is varied from 15 MPa to 11.7 MPa. Test CT-17 was an attempt to look at an even lower differential stress (2 MPa), but a horizontal fracture developed connecting with what appeared to be an open bedding plane.

The pressure-time curves for tests in Devonian shale are contained in Appendix B. It should be noted that the fracture extension pressures for CT-10 and CT-16 are within 1 or 2 MPa of the least principal stress (5 MPa), whereas for CT-15 the fracture extension pressure is 10 MPa above the least principal stress. It is possible that the low values for CT-10 and CT-16 are a result of the hydraulic fracture having propagated unstably to the boundary immediately after breakdown with the subsequent extension pressure simply involving pumping fluid through the fracture to the boundary.

The hydraulic fracture created in CT-10 was relatively uninterrupted by natural fractures (Figure 13) as compared to those created in CT-15 (Figures 14 and 15) and CT-16 (Figures 16, 17, and 18). Test CT-10 was also the test with the highest differential stress (15 MPa as compared to 5 MPa), which is probably a controlling factor in the degree of interaction, as discussed in the next section. The hydraulic fractures in CT-15 and CT-16 showed a much greater degree of interaction with the natural fractures. Examples of fracture arrest can be seen in Figures 14 and 16. Examples of hydraulic fractures being offset by natural fractures can be seen in Figures 15 and 17.

An example of fracture branching is shown in Figure 18. In Figures 14 and 15 there are clear instances of natural fractures that opened and took fluid in contrast to the surrounding dry material.

One aspect of the hydraulic fractures in Devonian shales that was difficult to photograph was the nature of the fracture trace in a vertical plane. While the overall trend of the trace was vertical, there were numerous horizontal offsets along bedding planes.



Figure 13. Test CT-10.



Figure 14. Fracture arrest in test CT-15.



Figure 15. Fracture offset in test CT-15.



Figure 16. Fracture arrest in test CT-16.

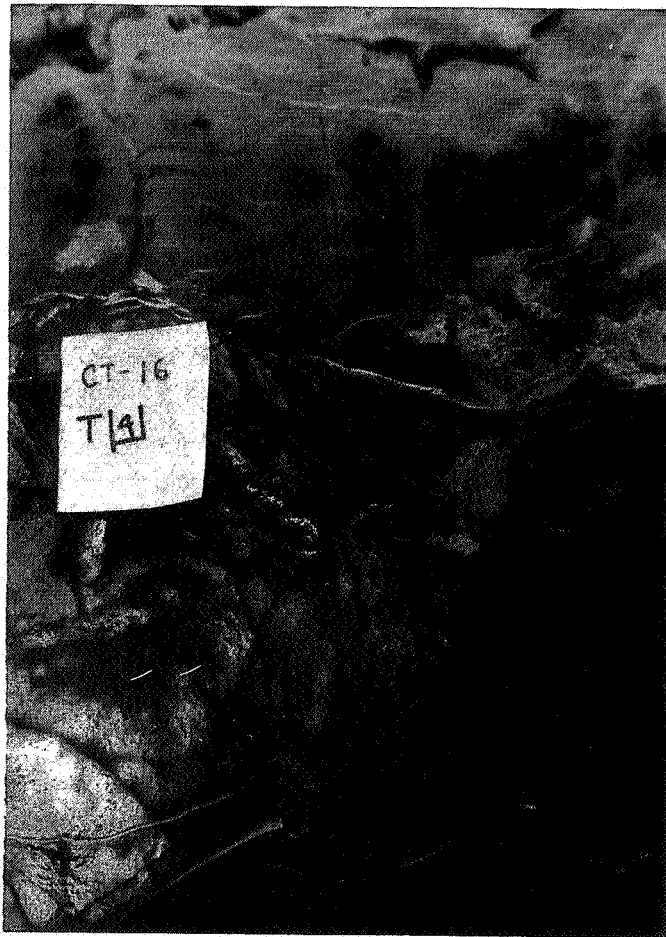


Figure 17. Fracture offset in test CT-16.



Figure 18. Fracture branching in test CT-16.

SECTION 3. ANALYSIS

3.1. Theoretical Considerations

A simple theoretical description of the interaction between a hydraulic fracture and a pre-fracture has been developed to act as a guide for further experimentation and as a basis for extrapolating the results to the field. Conceivably three things can happen when a hydraulic fracture reaches a pre-fracture: it can open the pre-fracture (Figure 19A), it can be arrested (Figure 19B), or it can cross the pre-fracture (Figure 19C). From the experiments it can be seen that all three things do actually occur, but each under different conditions.

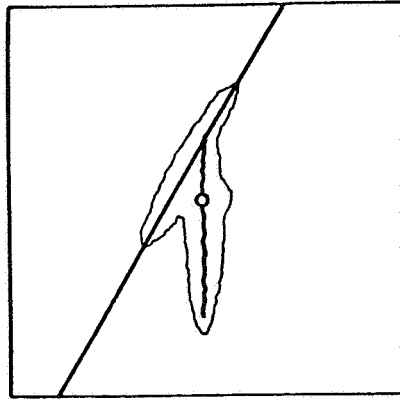
The critical situation is illustrated in Figure 20. Here a hydraulic fracture has just reached a pre-fracture, and the wings of the hydraulic fracture have grown to equal length, L . A simplifying assumption made in this development is that the wing intersecting the pre-fracture can be treated as an open channel through which the fluid pressure is transmitted to the point of intersection.

If the fluid pressure at the time of intersection is greater than the normal stress, σ , on the pre-fracture then the pre-fracture should open (Figure 19A). In order to develop a criterion for when this opening will occur, we need to calculate the pressure, p , in a penny-shaped fracture of radius L . This can be done using Sneddon's relation as follows:

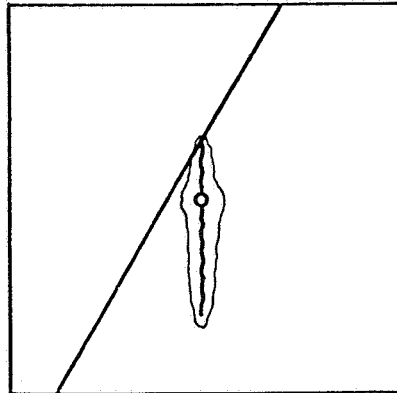
$$p - \sigma_{\min} = \left[\frac{\pi EG}{4(1-\nu^2)L} \right]^{\frac{1}{2}} \quad (2)$$

where E is Young's modulus, G is fracture energy, and ν is Poisson's ratio. To obtain an analytic expression for the opening criterion the pressure, p , given by Equation 2, is set equal to the normal stress, σ , given by Equation 1, as follows:

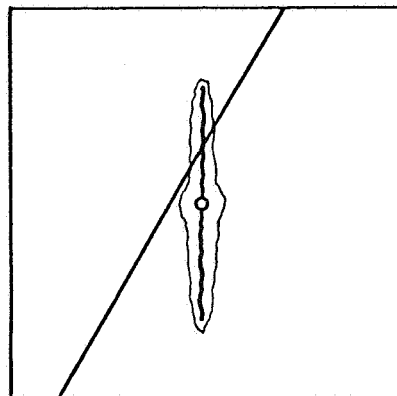
$$\left[\frac{\pi EG}{4(1-\nu^2)L} \right]^{\frac{1}{2}} + \sigma_{\min} = \sigma_{\max} \sin^2\theta + \sigma_{\min} \cos^2\theta$$



A. Open



B. Arrest



C. Cross

Figure 19. Types of interaction between hydraulic fractures and pre-fractures.

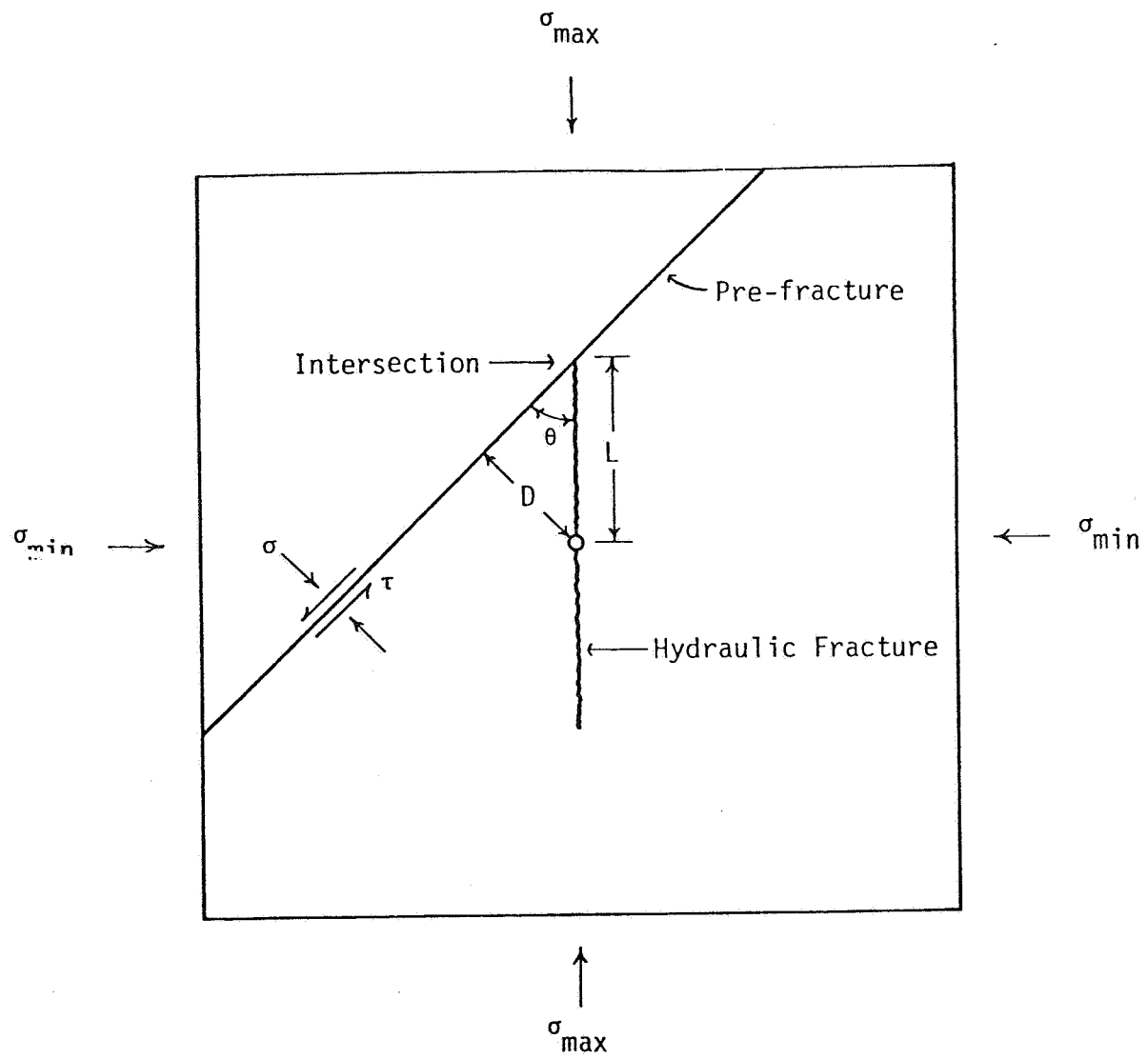


Figure 20. Diagram of hydraulic fracturing experiment in pre-fractured hydrostone at critical point of intersection.

Rearranging this, one obtains the following expression for the critical horizontal differential stress as a function of pre-fracture angle:

$$\sigma_{\max} - \sigma_{\min} = \frac{\left[\frac{\pi EG}{4(1-\nu^2)L} \right]^{1/2}}{\sin^2\theta} \quad (3)$$

If the pressure in the fracture at the time of intersection is less than the normal stress, then the pre-fracture should remain closed. However, the normal stress may be lowered by a pore pressure effect enough to allow slip, especially if the shear stress, τ , on the pre-fracture is high. To establish a criterion for conditions under which slip might occur, the normal stress in a linear sliding friction criterion is reduced by the pressure in the fracture as follows:

$$\tau = \mu (\sigma - p) \quad (4)$$

where μ is the coefficient of friction. Using the expression for shear stress on a plane at angle θ and Equations 1 and 2, Equation 4 becomes:

$$\frac{\sigma_{\max} - \sigma_{\min}}{2} \sin 2\theta = \mu \left\{ \sigma_{\max} \sin^2\theta + \sigma_{\min} \cos^2\theta - \left[\frac{\pi EG}{4(1-\nu^2)L} \right]^{1/2} - \sigma_{\min} \right\}$$

Rearranging this, an expression for differential stress as a function of θ can be obtain as follows:

$$\sigma_{\max} - \sigma_{\min} = \frac{\left[\frac{\pi EG}{4(1-\nu^2)L} \right]^{1/2}}{\frac{\sin^2\theta}{2} - \mu \sin^2\theta} \quad (5)$$

If shippage occurs, then the crack tip will be blunted, thus arresting growth in that direction (Figure 19B). If slippage does not occur, then continuity will be maintained across the pre-fracture and the hydraulic fracture should cross the pre-fracture.

3.2. Comparison Between Theory and Experiment

Equations 3 and 5 represent limits for certain types of interaction between hydraulic and pre-existing fractures. The curve determined by Equation 3 separates combinations of horizontal differential stress ($\sigma_{\max} - \sigma_{\min}$) and angle of approach (θ) for which the pre-fracture will open from those for which it will remain closed. In the same manner Equation 5 separates combinations for which slippage will occur from those for which slippage will not occur. In order to compare these limiting curves to the results of the experiments, E , ν , G , L , and μ must be specified.

Values used for the elastic constants are as follows:

$$E = 10 \text{ GPa} \quad (1.45 \times 10^6 \text{ psi})$$

$$\nu = 0.22$$

Young's modulus (E) was determined by running uniaxial compression tests on hydrostone (35/100). The value for Poisson's ratio was taken from a study by Haimson and Fairhurst (1969).

Two methods were used in an attempt to gain a measure of fracture energy. The first was to perform four-point bending tests on notched rods. Fracture propagation in these tests was unstable and did not yield reliable results. The second was to use data from the hydraulic fracturing experiments in Equation 2 and solve for G . The fractures produced in tests CT-2, CT-3a, CT-3b, and CT-8 were relatively symmetrical and therefore are the best to use in Sneddon's equation for a penny-shaped crack. The pertinent data from the tests and the results of the calculation are presented in Table 4. It appears that G may be highly variable. The influence of this variability on theoretical plots will be discussed later in the section when parameter-sensitivity is discussed.

Fracture radius (L) as it appears in Equations 3 and 5 represents the distance along the hydraulic fracture from the wellbore to the pre-fracture. However, the distance held constant in the tests was the distance (D) between the wellbore and the pre-fracture measured

Table 4. Fracture energies for hydrostone calculated from hydraulic fracturing experiments.

<u>Test No.</u>	<u>P - σ_{min} (MPa)</u>	<u>Average Fracture Radius (cm)</u>	<u>Fracture Energy G (J/m²)</u>
2	13.0 - 10 = 3.0	7.30	78.5
3a	14.2 - 10 = 4.2	6.17	129.8
3b	14.7 - 10 = 4.7	6.62	174.4
8	6.8 - 5 = 1.8	7.86	30.4

perpendicular to the pre-fracture. L is in fact a function of θ , as can be seen in Figure 20. Therefore in plotting Equations 3 and 5, the following substitution is made for L :

$$L = \frac{D}{\sin\theta}$$

In general D was 2.5 cm (~1 in). The effects of variations in D will be considered later.

The coefficient of friction (μ) for hydrostone has not been measured in this study, and no data has been found in other works. However, most values for μ for rocks or rock-like materials range from 0.5 to 1.0. The effect of changes within this range will be considered in the following discussion of parameter sensitivity.

The results of the experiments are compared to the limits determined by Equations 3 and 5 in plots of horizontal differential stress vs. angle of approach. For each test the result is indicated by the following symbols:

- o - hydraulic fracture opened pre-fracture.
- T - hydraulic fracture was arrested by pre-fracture.
- x - hydraulic fracture crossed pre-fracture.

In Figure 21 the results are compared to plots of Equation 3 for three different values of G (20, 70 and 120 J/m²). As discussed earlier Equation 3 is theoretically the limit beyond which the pre-fracture should not open. The value of 20 J/m² appears to be too low from the viewpoint of both the results and the values given in Table 4. Values of 70 and 120 J/m² are more in line with the values calculated in Table 4, and one can see a tendency for the curves corresponding to these values in Figure 21 to lie between points indicating an open pre-fracture and those indicating arrest of a hydraulic fracture.

The effect of changes in G on Equation 5 are illustrated in Figure 22. If the assumptions made in deriving this equation have some validity, then the appropriate curve should divide points indicating hydraulic fracture arrest from points indicating that the

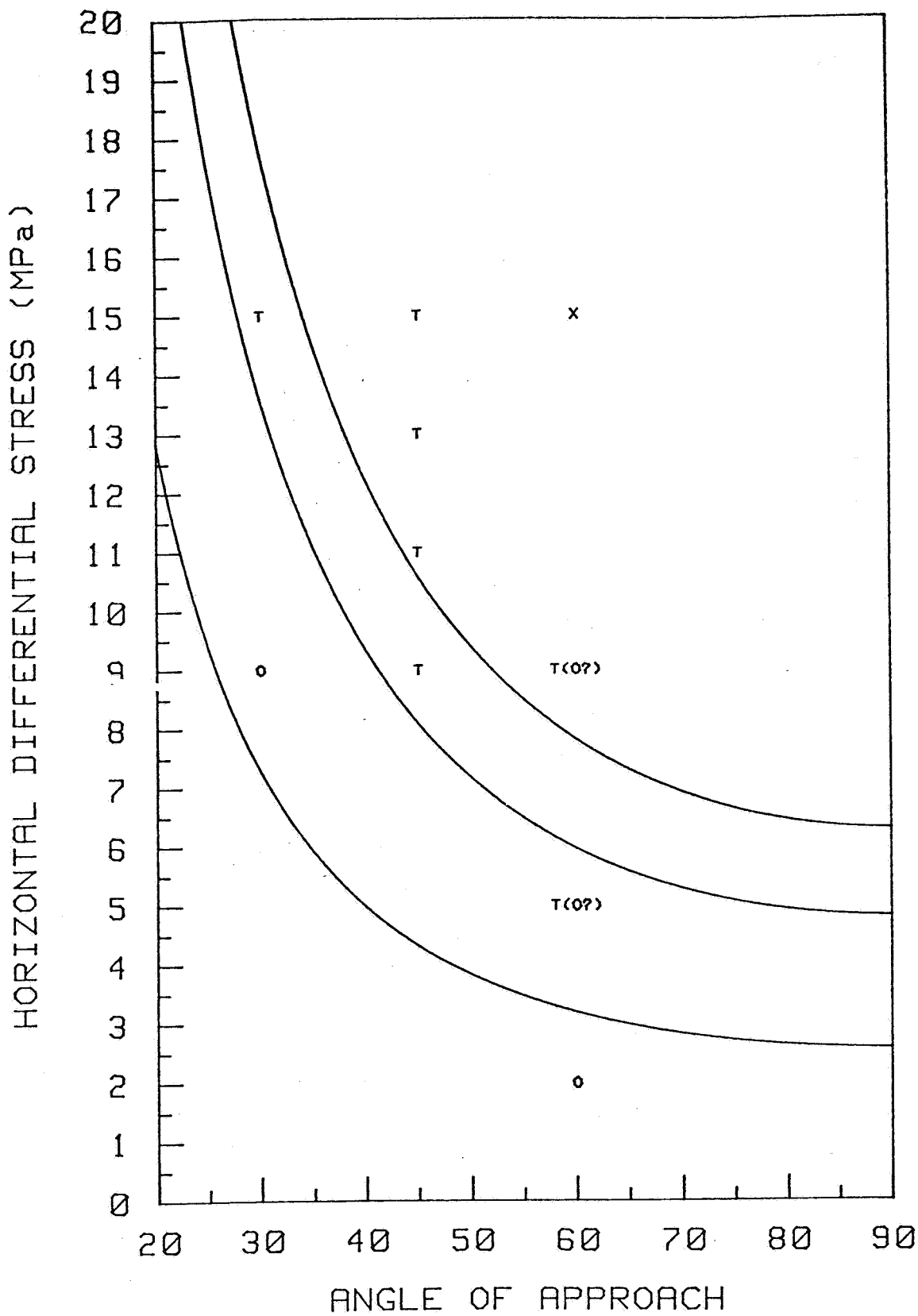


Figure 21. Theoretical limits of pre-fracture opening (Equation 3) for three values of G (20, 70, 120 J/m^2) increasing from bottom to top.

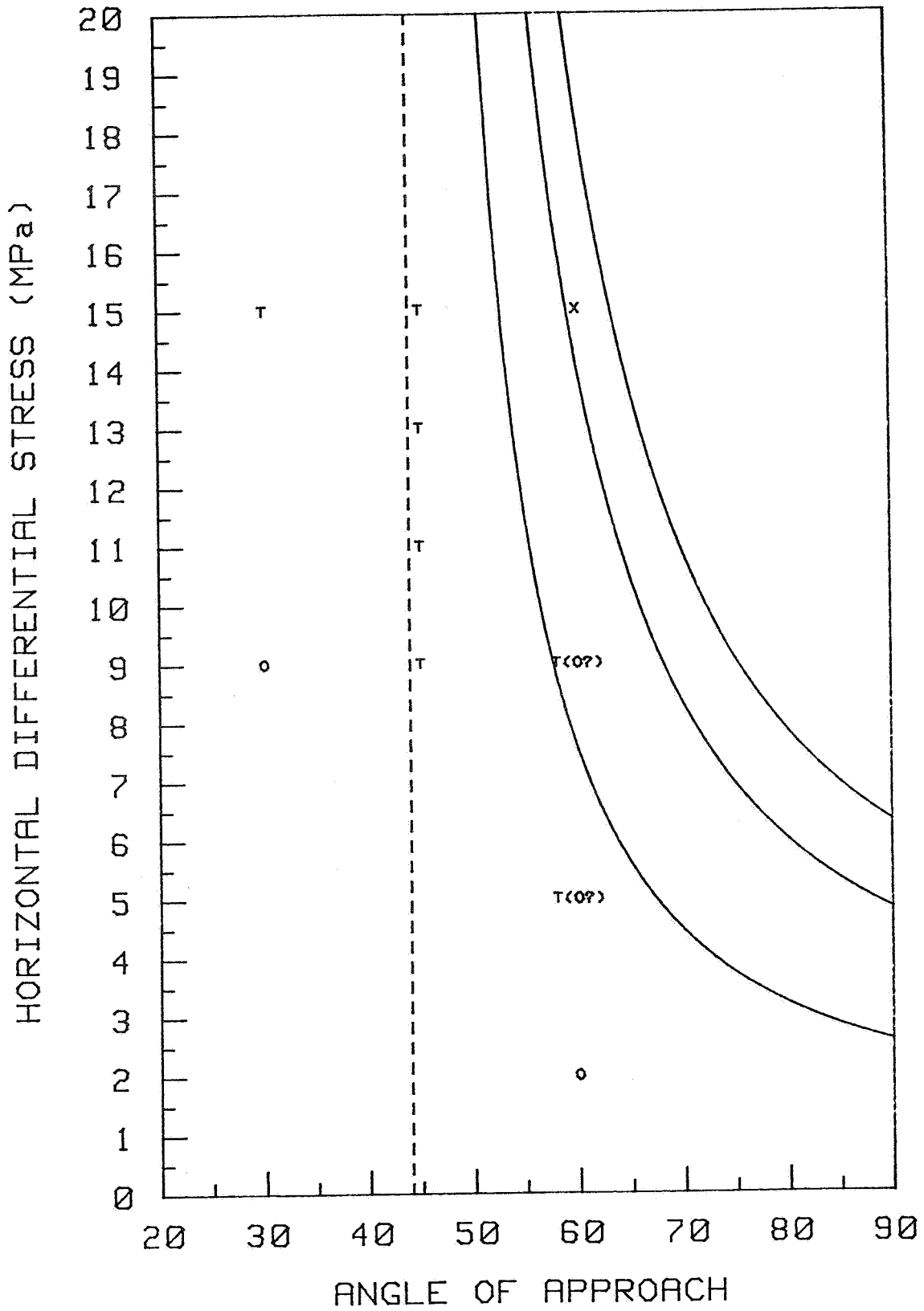


Figure 22. Theoretical limits of hydraulic fracture arrest (Equation 5) for three values of G (20, 70, and 120 J/m²) increasing from bottom to top.

hydraulic fracture crossed the pre-fracture. The latter result occurred in only one test; however, the point for this test falls on the correct side of two of the curves in Figure 22. More important, all but one of the points indicating fracture arrest fall on the correct side of all three curves, and the one exception falls on the correct side of two curves.

The coefficient of friction affects only Equation 5. Its influence is not strong, as can be seen in Figure 23. The values of μ used in plotting these curves were 0.50, 0.75 and 1.0. All of the points indicating fracture arrest fall on the correct side of all three of these curves. The one point indicating fracture crossing falls on the correct side of only one curve.

The influence of changes in D are shown in Figure 24. In some tests D was approximately 1.7 cm (0.67 in) instead of 25 cm (1 in). As can be seen, the effect of this difference is not great.

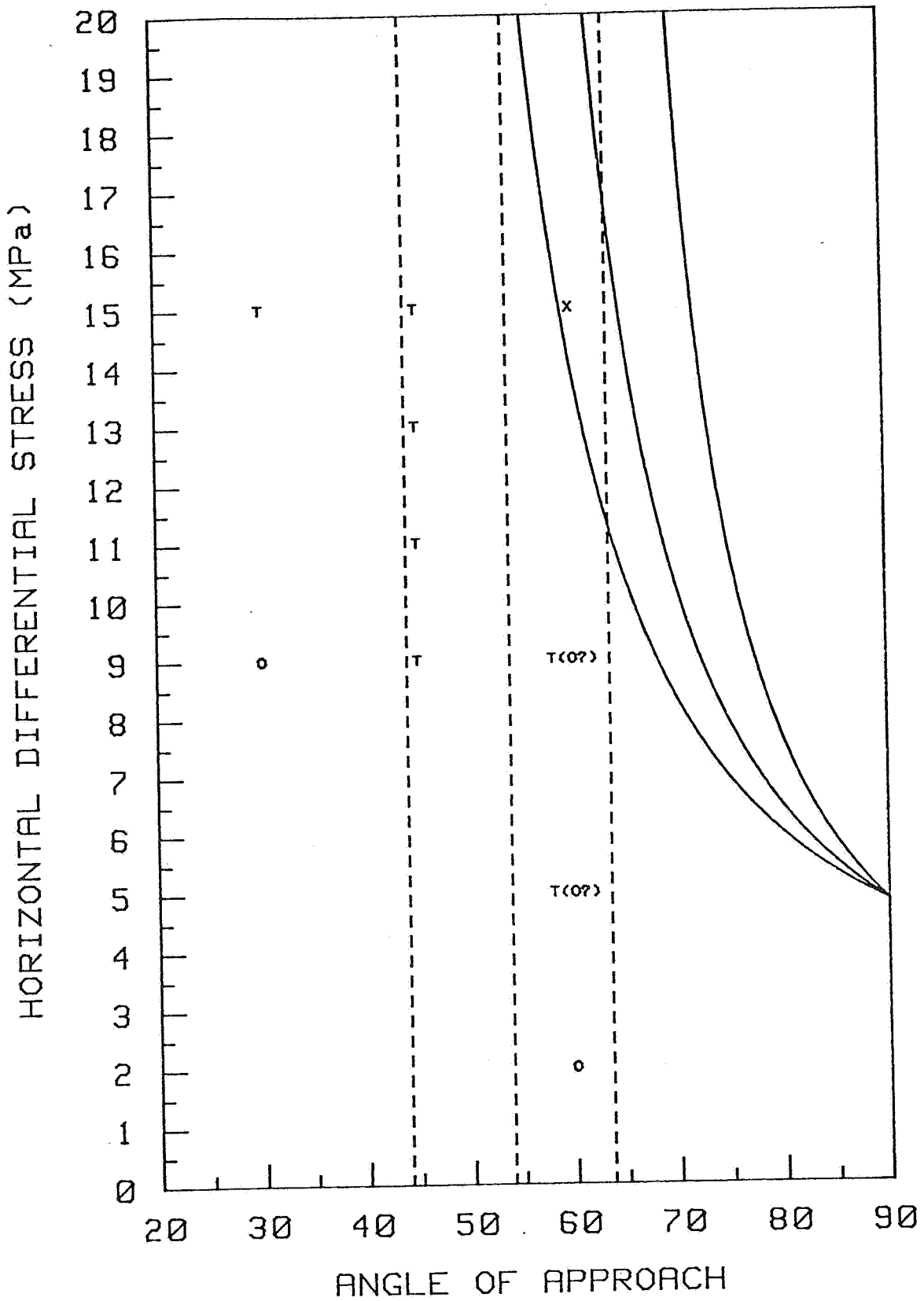


Figure 23. Theoretical limits of hydraulic fracture arrest for three values of μ (0.50, 0.75, and 1.00) increasing from right to left.

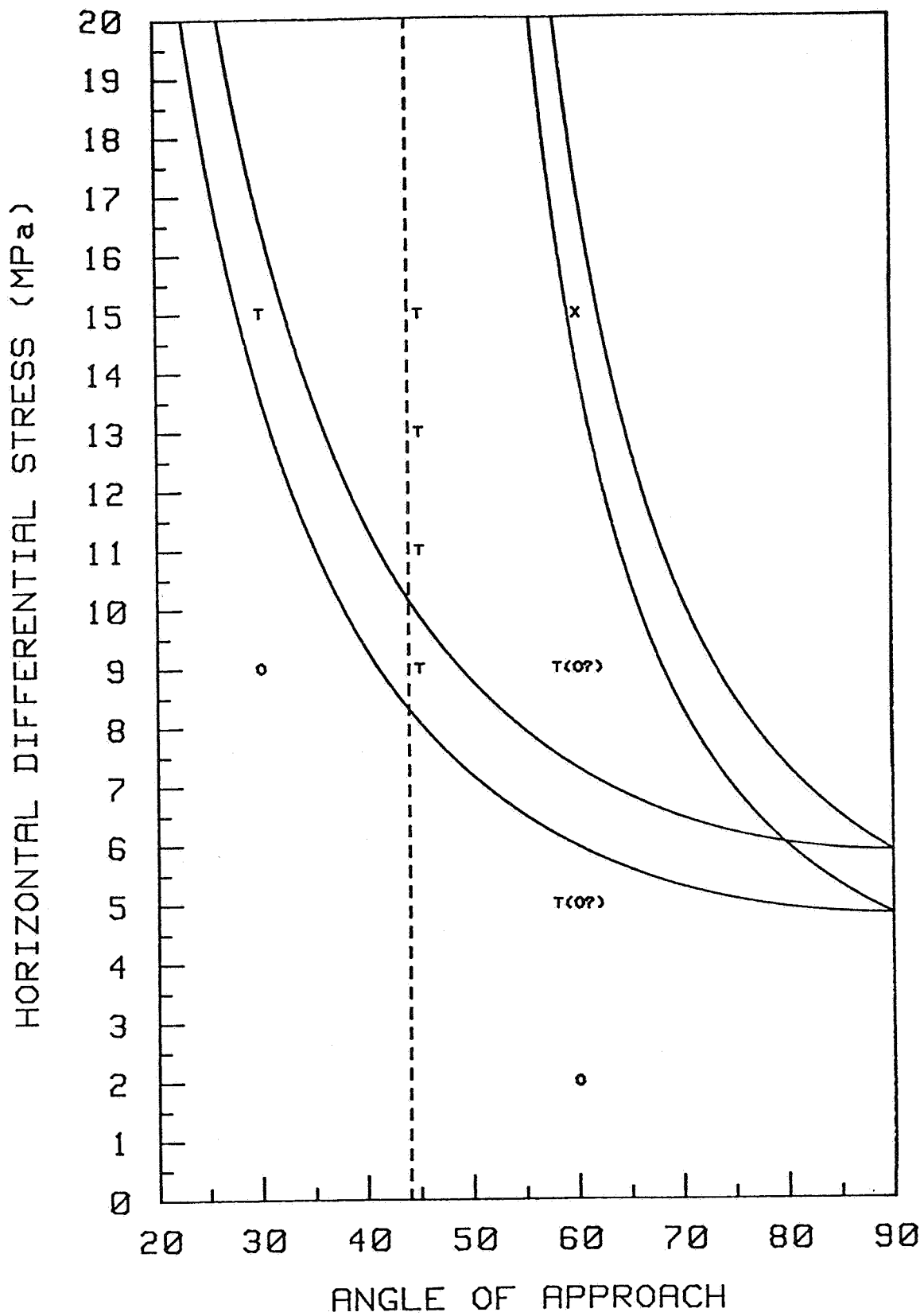


Figure 24. Influence of changes in D on Equations 3 and 5. $D = 2.5$ cm for upper set and 1.7 cm for lower set.

SECTION 4. CONCLUSION

Obviously more experimental work is needed before the theory developed in subsection 3.1 can be confirmed. Nevertheless, there is a general conclusion pointed to by the experiments in both hydrostone and Devonian shale as well as by the theory, and it is that the morphology of hydraulic fractures tends to be dominated by natural fractures.

The strong influence of natural fractures can be seen qualitatively in the photographs of the experiments in Devonian shale. The influence of pre-fractures is demonstrated in a more quantitative manner by the experiments in hydrostone. In nine out of ten tests the hydraulic fracture was truncated by the pre-fracture. The one case in which the hydraulic fracture crossed the pre-fracture, and essentially behaved as if the pre-fracture was not there, was under a combination of the highest horizontal differential stress (15 MPa or 2,175 psi) and highest angle of approach (60°).

Theory also suggests that for most combinations of horizontal differential stress and angle of approach a hydraulic fracture will be either arrested or diverted by a pre-existing fracture. Theoretically, this should be true even for low fracture energies and high coefficients of friction on the pre-existing fracture (see Figure 22 and 23). Fracture crossing was indicated by the theory only for high horizontal differential stresses and high angles of approach.

The implication of this study for hydraulic fractures in the field is that symmetrical, double-winged, vertical fractures are probably a rare occurrence in naturally fractured reservoirs. It would be more likely to have fractures with wings diverted at different angles or with truncated wings of different lengths.

Two points should be mentioned with regard to the interaction between bedding planes and hydraulic fractures in the Devonian shale blocks. First, in the vertical direction the hydraulic fractures tended to be offset by bedding planes producing a step-like morphology. Second, the hydraulic fractures tended to be contained in the vertical direction producing a rectangular fracture rather than a penny-shaped or elliptical fracture.

ACKNOWLEDGEMENTS

I wish to thank Dr. Chapman Young for many helpful discussions and advise throughout the project. Gratitude is also due Mrs. Nancy C. Patti for her help in design and construction of the test apparatus. Special thanks are due Mr. Steven A. Dischler for his assistance in preparing specimens, running experiments and reducing data. Additional thanks are due Miss Page Lamberson for proofing and typing the final manuscript. This work was supported by the Department of Energy through their Morgantown Energy Technology Center.

REFERENCES

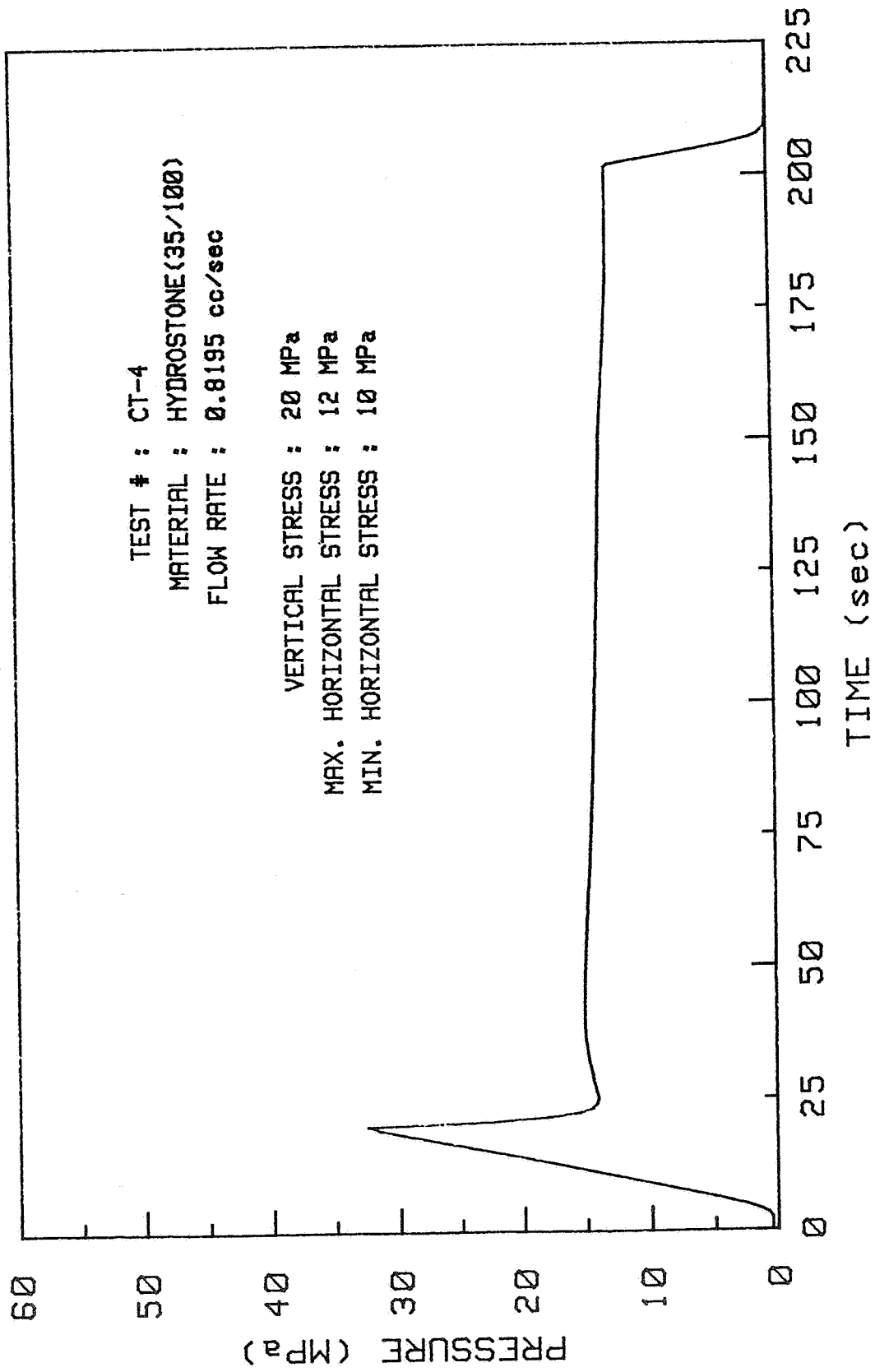
Haimson, B., and Fairhurst, C., "Hydraulic Fracturing in Porous-Permeable Materials," J. Pet. Tech. (July, 1969), pp. 811-817.

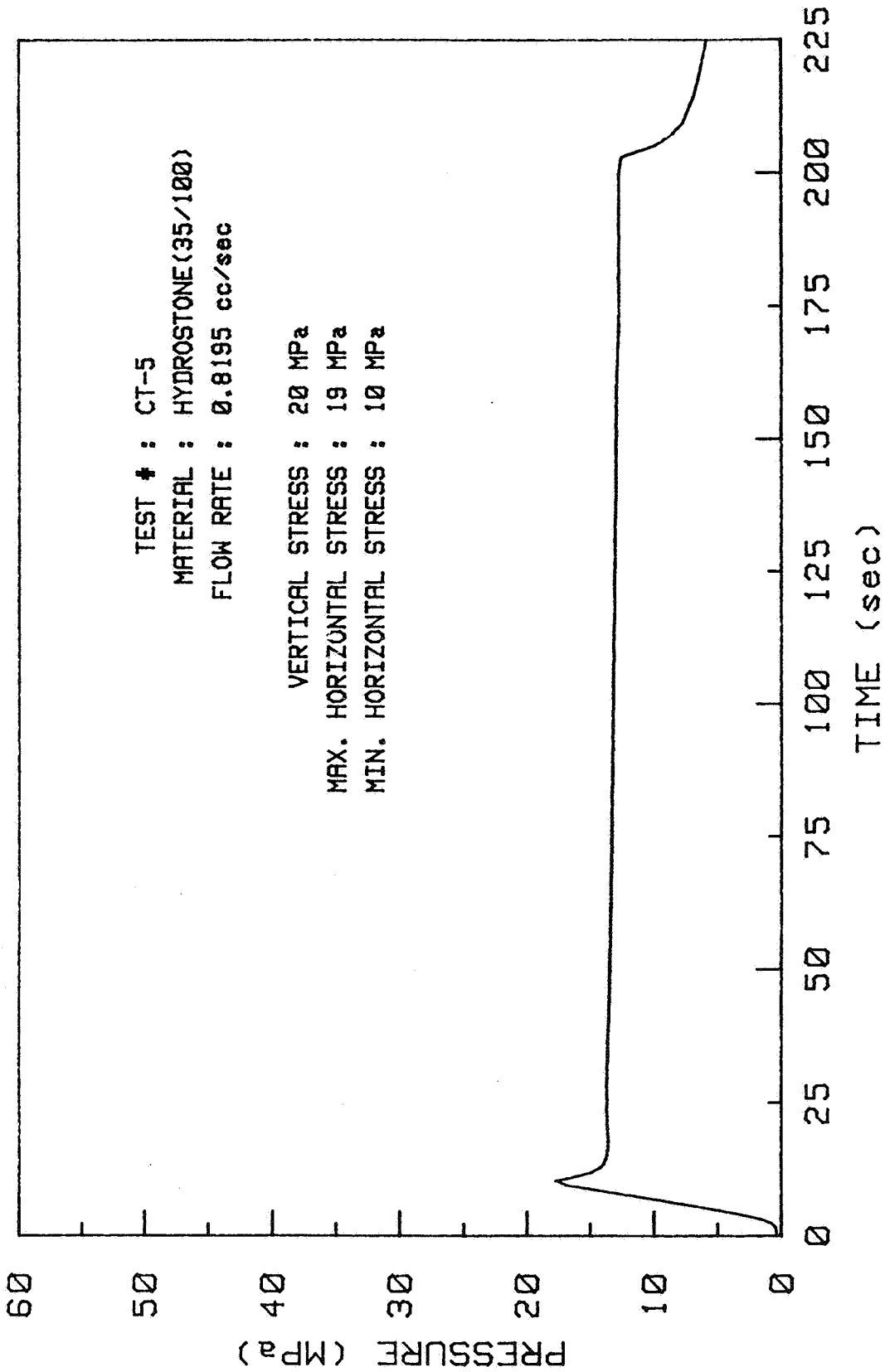
Hanson, M. E., Shaffer, R. J., and Anderson, G. D., "Effects of Various Parameters on Hydraulic Fracturing Geometry," Soc. Pet. Eng. J. (August, 1981), pp. 435 - 443.

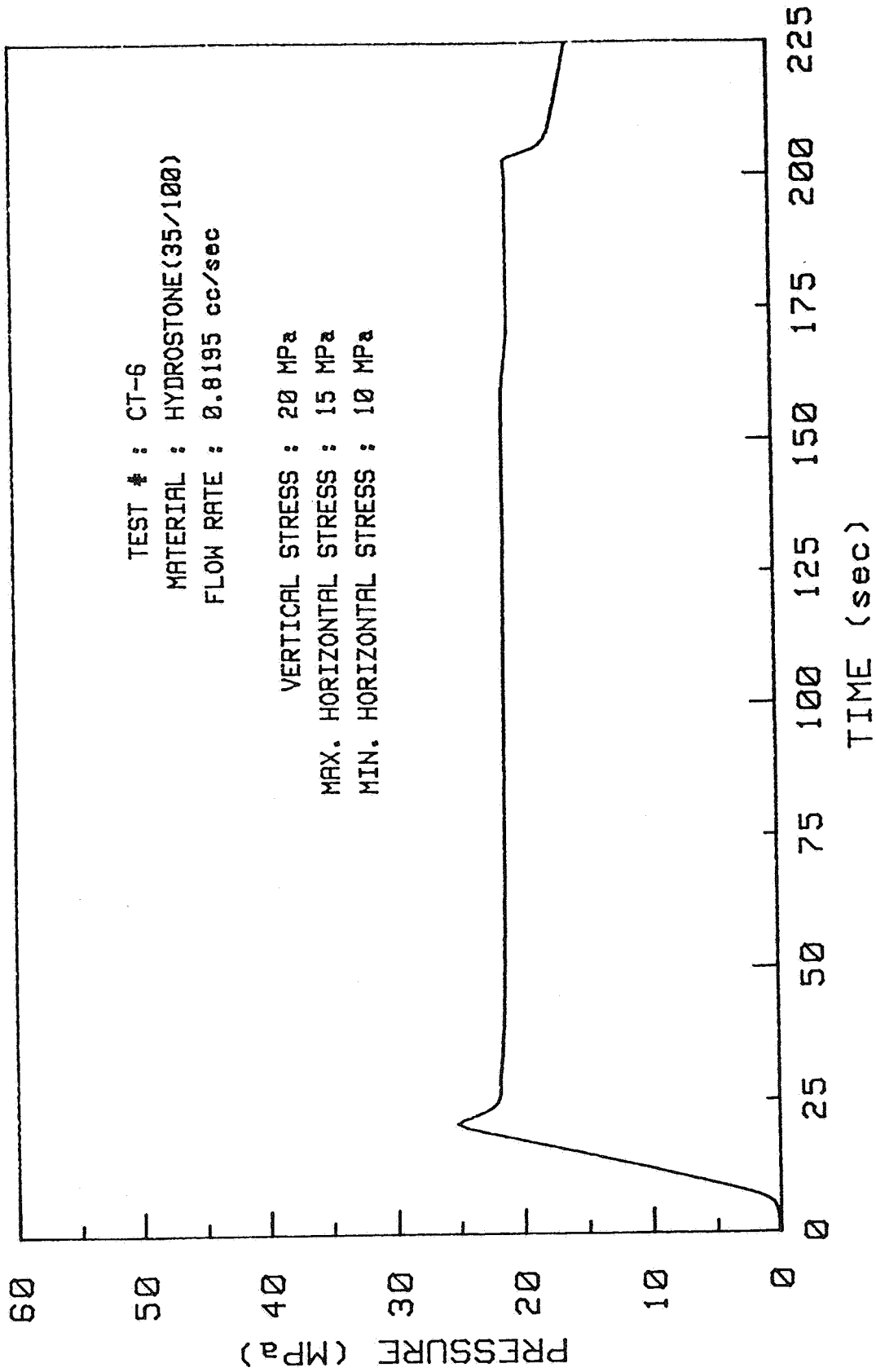
Sneddon, I. N., "The Distribution of Stress in the Neighborhood of a Crack in an Elastic Solid," Proc. Roy. Soc. London, v. A-187, 1946, pp. 229 - 260.

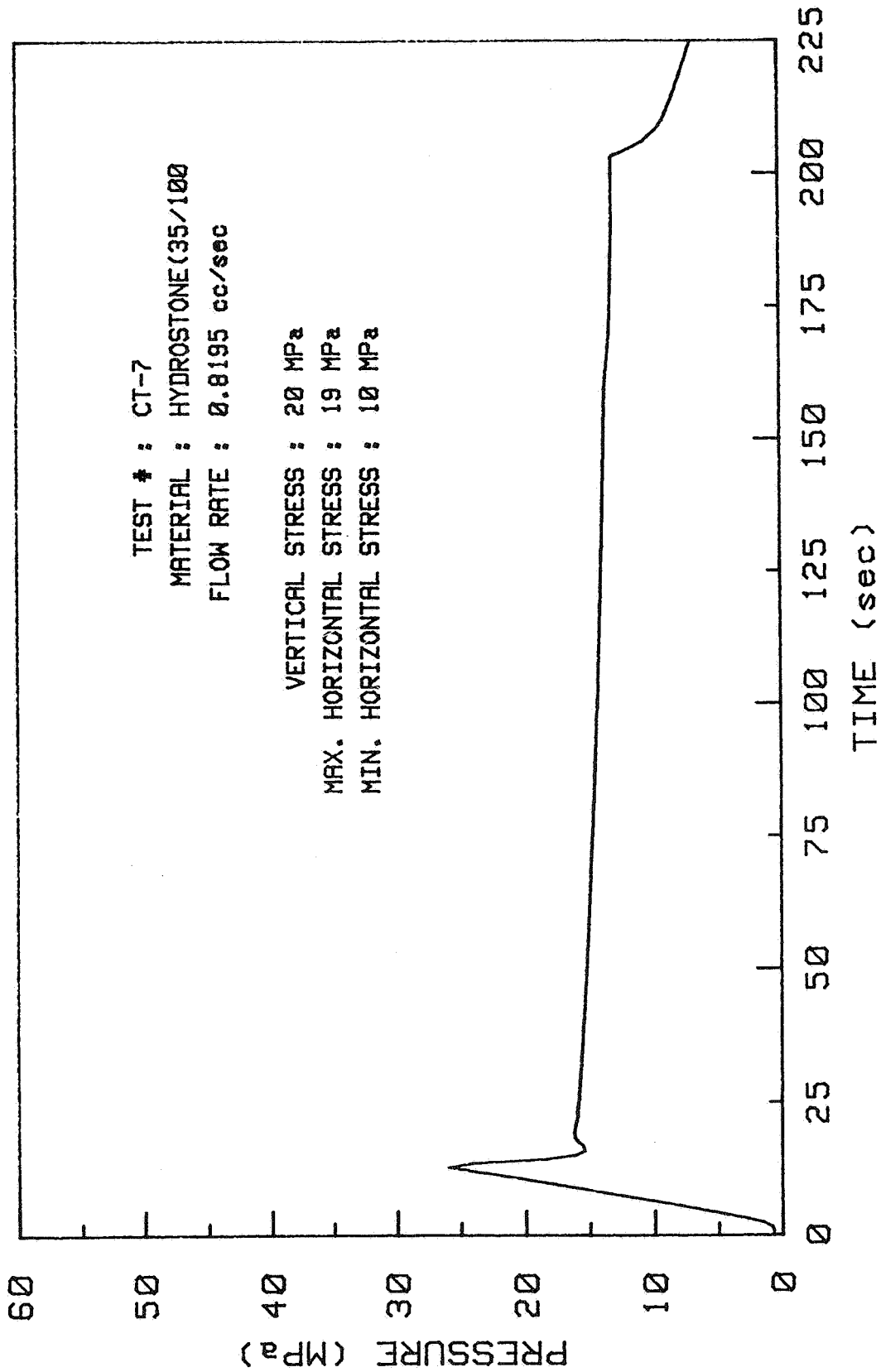
APPENDIX A:

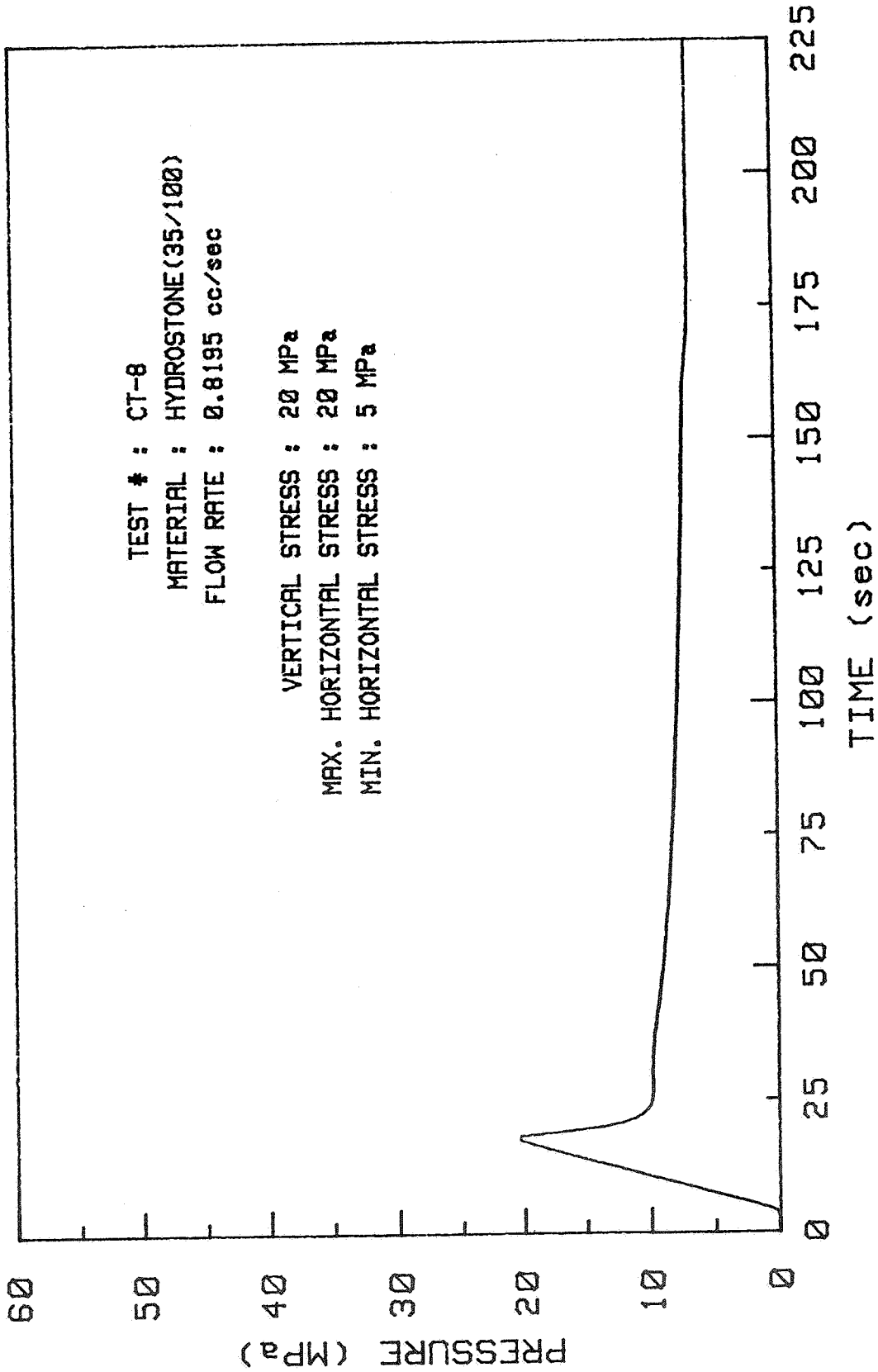
Pressure-Time Plots for Tests in Pre-Fractured Hydrostone

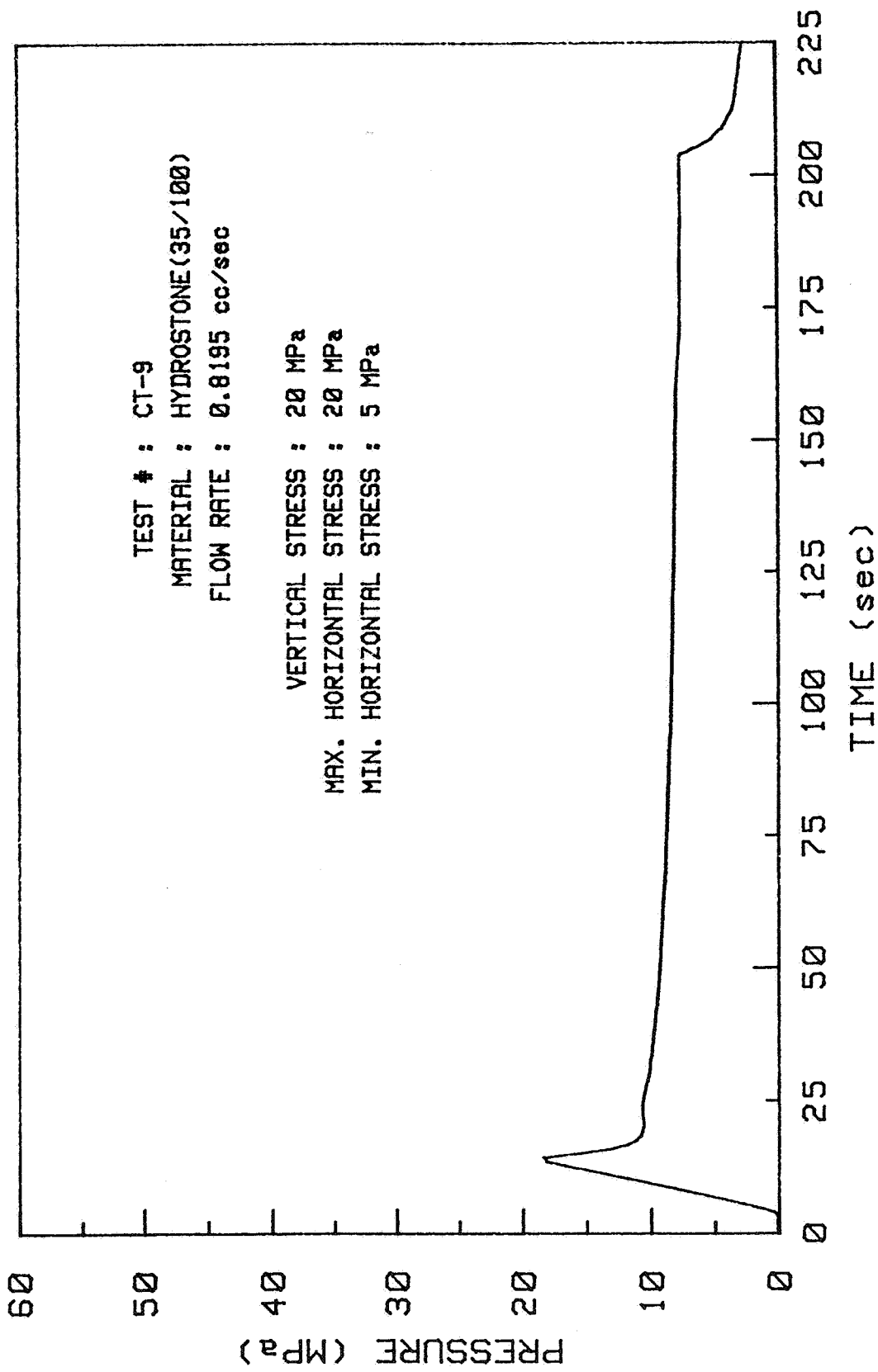


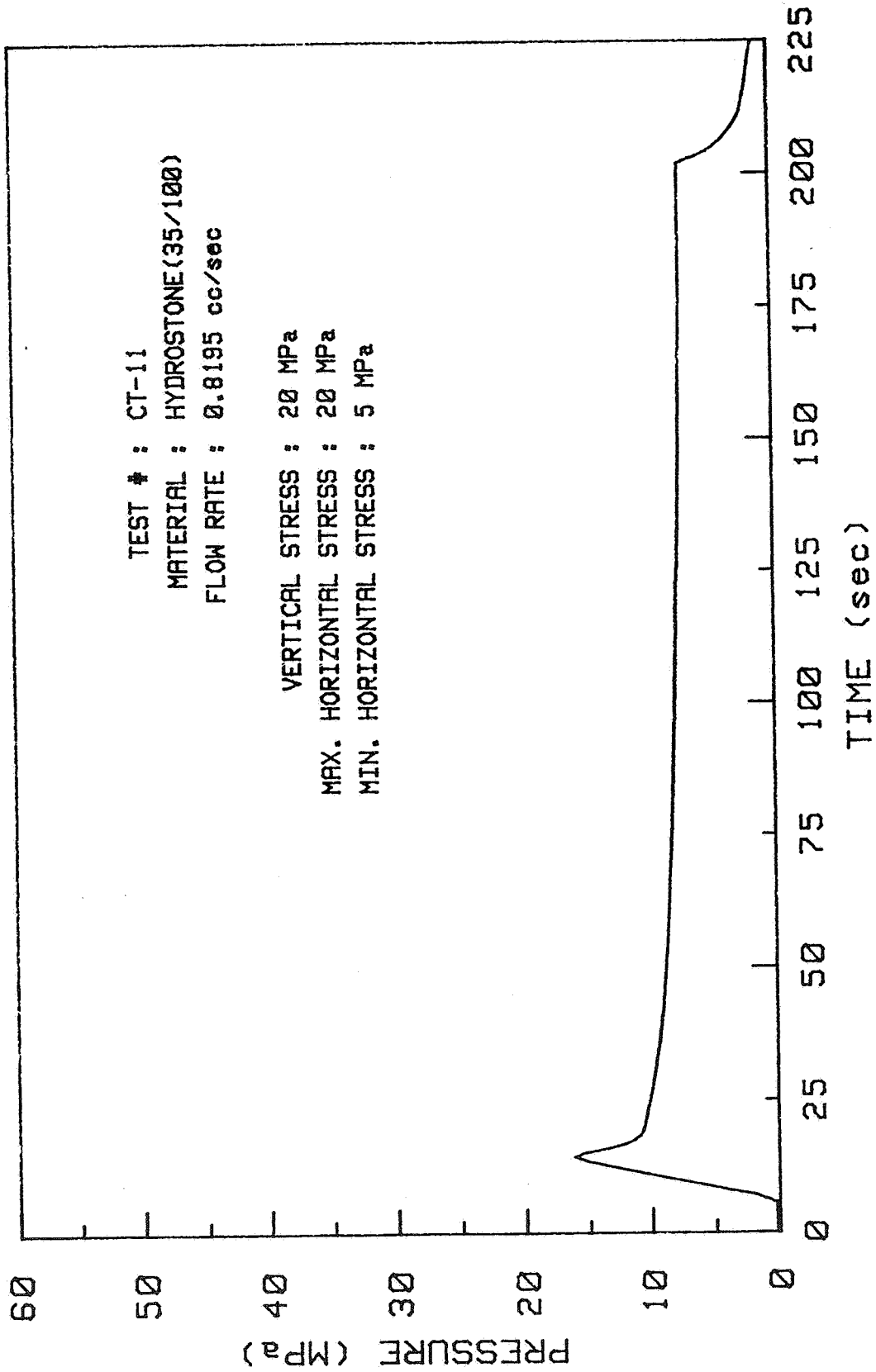


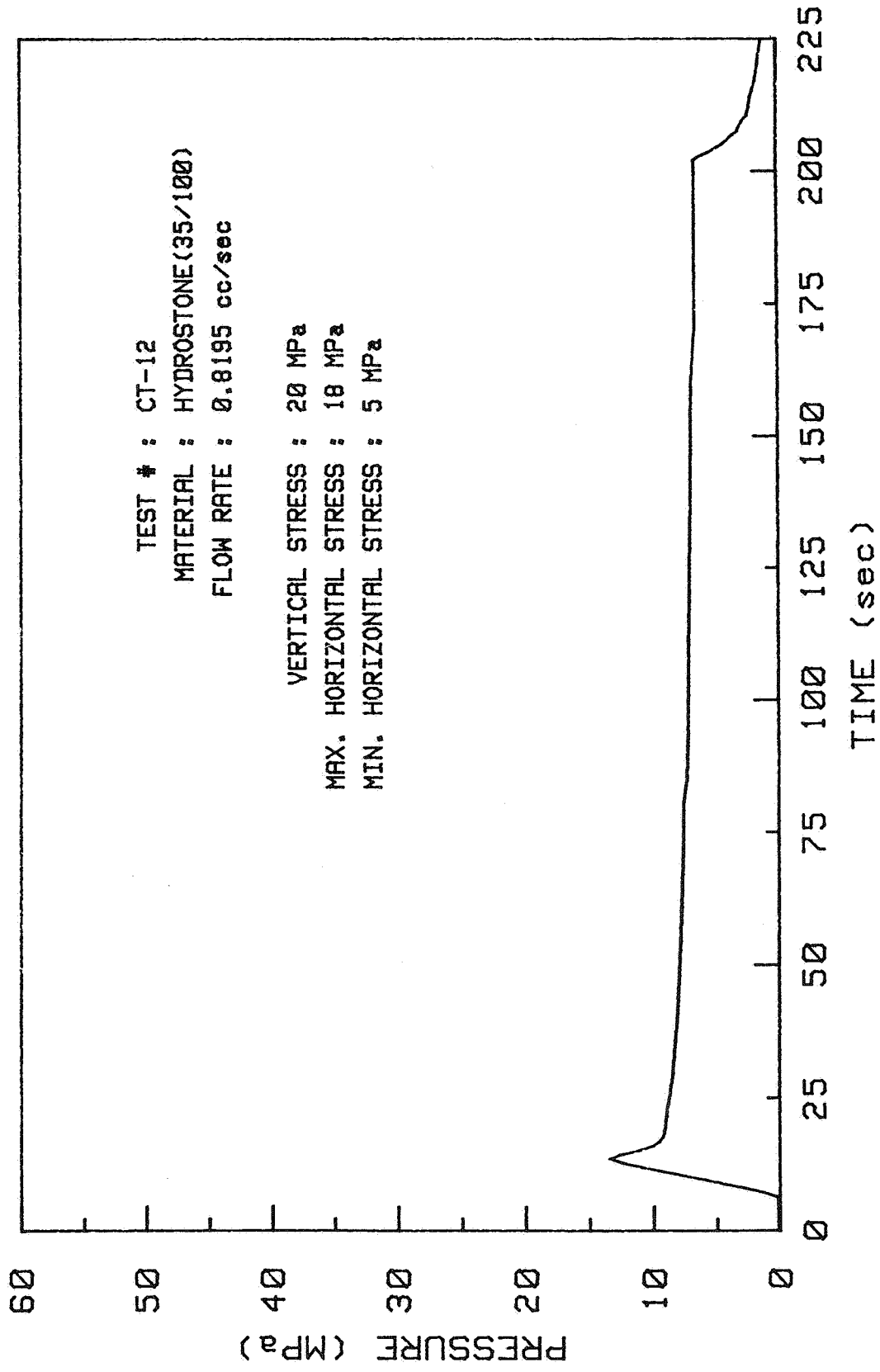


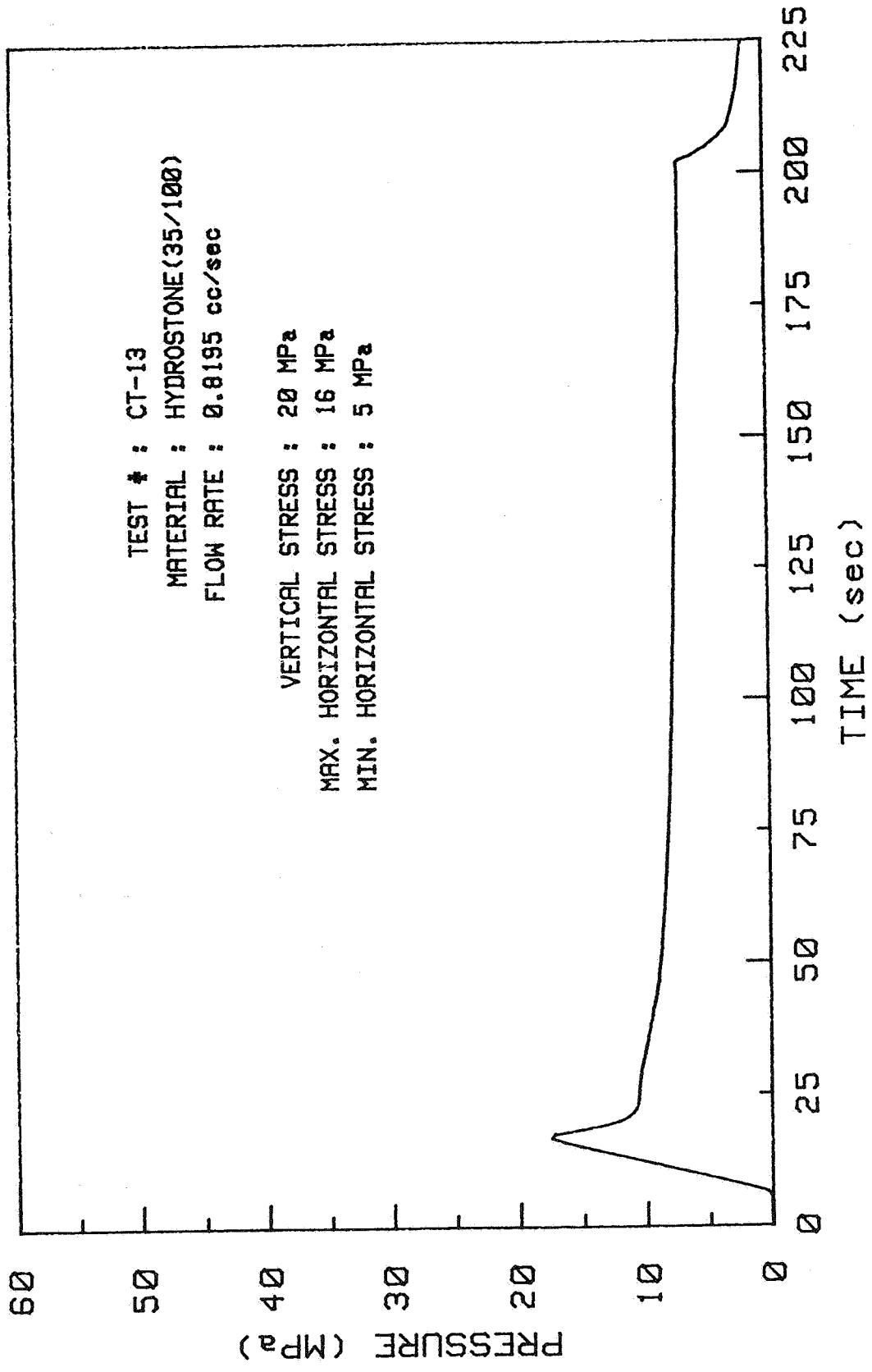


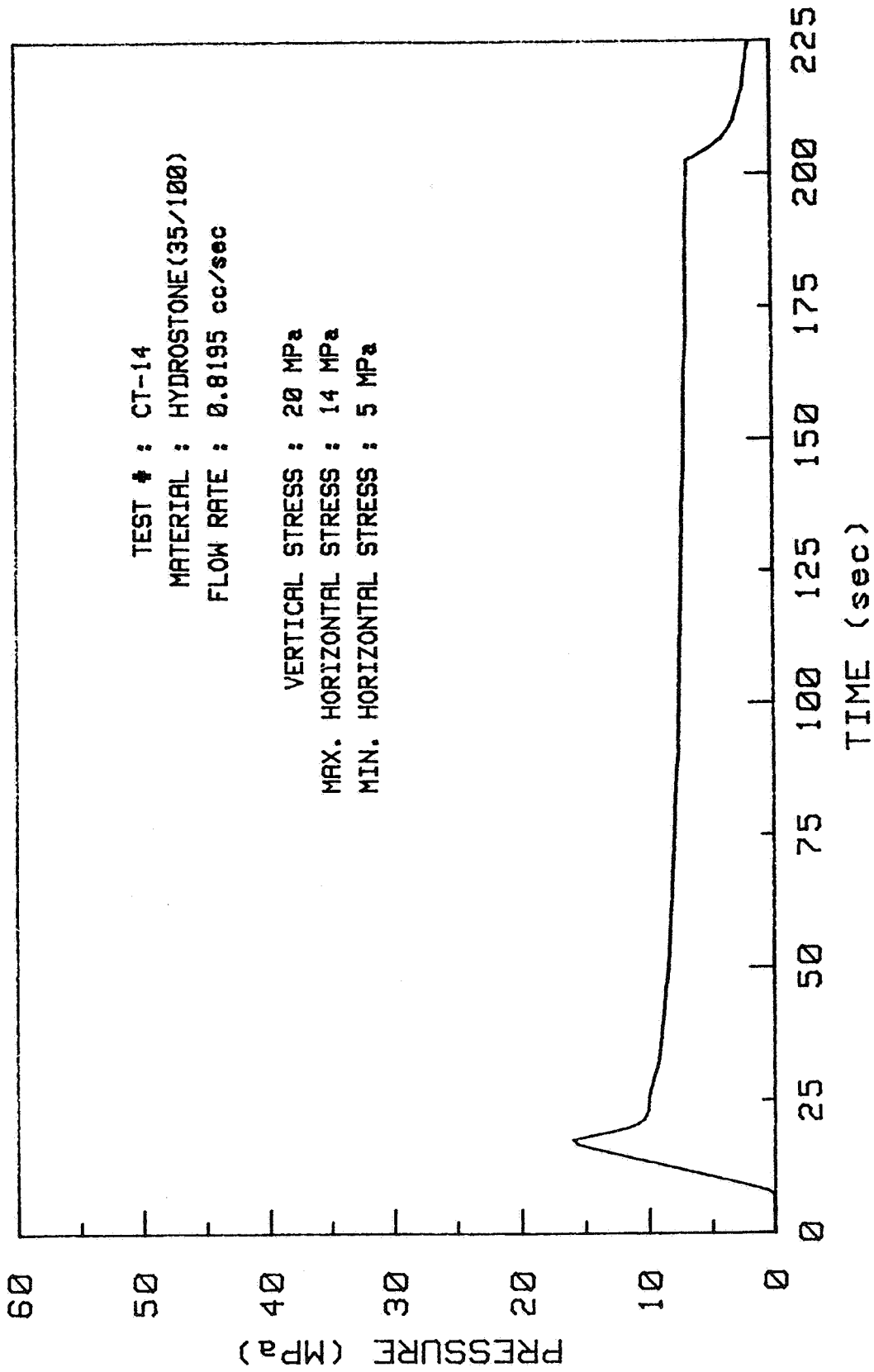












APPENDIX B:
Pressure-Time Plots for Tests in Devonian Shale

